*"This is the peer reviewed version of the following article: Christoph Ziegler, André Wolf, Wei Liu, Anne-Kristin Herrmann, Nikolai Gaponik and Alexander Eychmüller (2017). Modern Inorganic Aerogels. Angewandte Chemie-international Edition, 2017, Vol. 56, Issue 43, pp. 13200-13221, which has been published in final form at DOI:10.1002/anie.201611552.*


# Modern Inorganic Aerogels

**Christoph Ziegler, André Wolf, Wei Liu, Anne-Kristin Herrmann, Nikolai Gaponik and Alexander Eychmüller**

Physical Chemistry, Technische Universität Dresden, Bergstr. 66b, 01062 Dresden, Germany

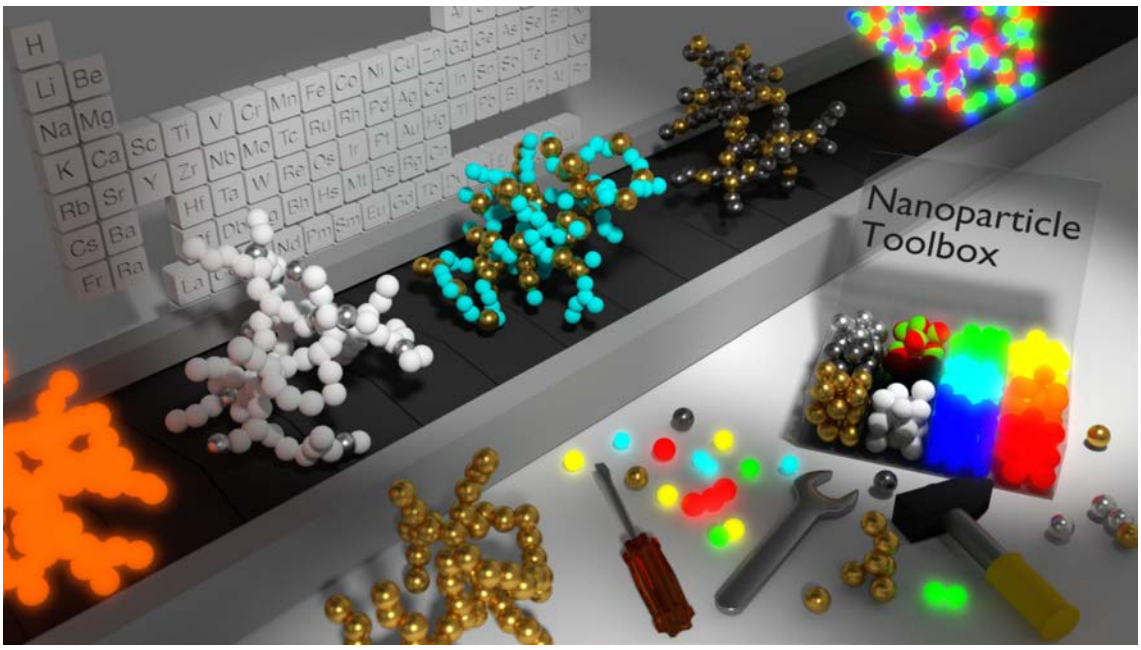


There is a huge variety of colloidal nanoparticles available -

Now we can use them to make something big!

## Abstract

Essentially, the term aerogel describes a special geometric structure of matter. It is neither limited to any material nor to any synthesis procedure. Hence, the possible variety of materials and therefore the multitude of their applications are almost unbounded. Here we present a comprehensive picture of the most promising developments in the field during the last decades.

## Introduction

Aerogels have record low density, large specific surface areas and can be made of almost any material. They are panoscopic materials with features smaller than 10 nm and a total monolith size of several centimeters. They can be conductive or insulating, transparent or perfectly black, chemically inert or super efficient catalysts, colorful and luminescent, magnetic and super absorbers. They already found applications in scientific areas like as part of Cherenkov detectors in particle accelerators or in space as NASAs Stardust collector as well as in everyday things like heat insulating materials in cycling gloves or rigidity enhancer in tennis racquets. Aerogels are the bridge between the nano and the macro world and their potential for new applications is almost unlimited.

The scientific story of aerogels started almost a century ago with a bet between two young scientists. Samuel Stephens Kistler argued that he could remove all the liquid in a jelly without any shrinkage. Winning his bet resulted in the invention of aerogels, which he published in the journal Nature in 1931 in just a half page.[1] There he already outlined that it should be possible to make aerogels out of almost any material.

But what is a gel or an aerogel? We know gels from several everyday products like gelatin in the kitchen, styling gel in the bathroom and glue gel from the workshop. So we intuitively have a feeling about what gels are. Scientifically speaking, the international Union of Pure and Applied Chemistry (IUPAC) defines a gel as a "non-fluid colloidal network or polymer network that is expanded throughout its whole volume by a fluid".[2] From there it is already obvious that a gel is not connected to any specific material or material class but rather is described as a special geometric structure of matter. The smallest features are in the colloidal (1-100 nm) region whereas the whole structure can expand over an unlimited size range. Generally, the structure is comparable to a three-dimensional sponge-like network.

Most gels are obtained from classical gelation, which is the "process of passing through the gel point to form a gel or network".[2] In other words, a solution of certain molecular precursors turns into a solid network, completely soaked with the liquid solvent covering the entire initial volume. The gel point is reached when the network has just formed throughout the whole volume. This can usually be determined by rheology measurements. Theoretically the viscosity of the just-formed gel material tends to infinity. Again, this is a definition, which focuses on physical properties rather than chemical properties. Hence, in principle gels can be made of any kind of material.

Very often the gel formation mechanism follows the sol-gel process, which is the "process through which a network is formed from solution by a progressive change of liquid

precursor(s) into a sol, to a gel, and in most cases finally to a dry network".[2] Here the precursors usually undergo a polymerization reaction to continuously form first a sol consisting of individual nanoparticles that subsequently arrange into the network structure. For inorganic oxidic gels like silica gels this is a condensation reaction. It should be emphasized that this process usually cannot be stopped and will always result in a gel structure. Besides, it also implies that a soluble precursor exists that can undergo a polymerization/condensation reaction to form the desired solid inorganic material. Overall this means that the classical gel formation mechanism is limited to a small number of materials, because the material that forms the sol, and later the solid network, is the same as the linking material.

Furthermore it is possible to obtain gels through flocculation of a pre-formed colloidal solution. Flocculation, also referred to as coagulation or aggregation, is the "process of contact and adhesion whereby dispersed particles are held together by weak physical interactions ultimately leading to phase separation by the formation of precipitates of larger than colloidal size". This process is by definition reversible and therefore separates it from aggregation. However, for a gel formation the transition to aggregation, thus not being reversible, is gradual and the final gel usually cannot be dissolve into a stable colloid again. A very similar structure is obtained in voluminous precipitates. This approach can be used for several inorganic oxides and difficulty soluble salts. Both methods - flocculation and precipitation - will result in different three-dimensional network structures than classic gels. The gels formed by a classical gelation are usually monolithic and span the entire volume of the initial precursor solution. In contrast, the gels, obtained from flocculation or precipitation, occupy just a part of the initial volume and are more flake-like than monolithic.

No matter what mechanism let to the final gel, the gel scaffold is completely soaked into a liquid solvent. Depending on the type of solvent the gels are referred to as: hydrogels (where the fluid surrounding a network is water), aquagels (hydrogels with a colloidal network as the solid phase), alcogels (where the liquid phase is an alcohol or a mixture of alcohols) and gels where the liquid phase is a polar organic solvent sometimes referred to as either lipo- or oleogels.[2] Independent of the nature of the solvent, just emphasizing that the network is embedded in a liquid, gels are called either lyo- (from Greek *lysis* for solution) or solvogels.

The key step to obtain an aerogel (from Greek *aer* for air) is to replace the solvent with air while retaining the three-dimensional structure. This is most commonly found as the explanation of aerogels in literature.[3-5] However, the definition suggested by IUPAC is different as they describe an aerogel as a "gel comprised of a microporous solid in which the

dispersed phase is a gas".[6] We believe this covers just a part of the aerogels, which are known to date and even the most prominent silica aerogels do not fall under this definition. Besides, also IUPACs definition of xerogels, which they describe as an "open network formed by the removal of all swelling agents from a gel", is not complete. Xerogel is derived from the Greek word *xeros*, which means dry. Hence, a xerogel will be formed when the liquid phase of the gel is removed by drying (see Figure 1). In this drying procedure the network usually shrinks significantly because of the strong capillary forces at the interface of the solvent meniscus and the network interface. Replacing the initial solvent with one that has a very low surface tension like acetone, diethyl ether or n-hexane can reduce this effect. Minimizing also the solid-liquid interactions can reduce the capillary forces even further. This can be achieved by using a hydrophobic solvent for drying of a solid network material whose surface is hydrophilic and vice versa.

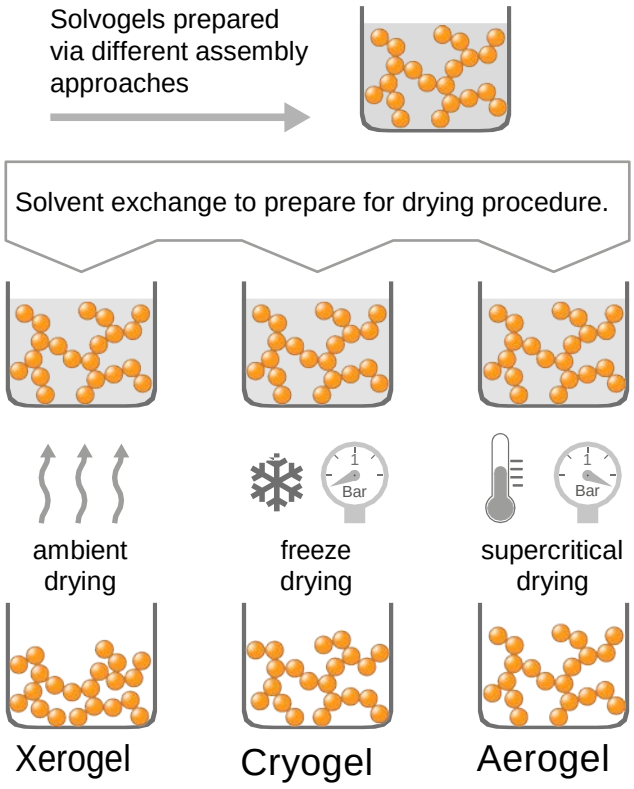


**Figure 1.** Drying procedures that determine the final state of the gel. A simple evaporation of the solvent present in the pores of the formed gel structure will result in a strong shrinkage of the network due to capillary forces (Xerogels). Freeze drying eliminates the capillary forces during the solvent removal. However, during the freezing of the solvent the network can be damaged (cryogels). A complete preservation of the nanostructured network can be achieved through supercritical drying (aerogels).

To retain the three-dimensional solid network from the solvogel two procedures are commonly used. One method is freeze-drying where the solvent in the gel will be frozen and subsequently the pressure of the surrounding will be reduced. If chosen appropriately, the solvent (like water, *tert*-butyl alcohol or cyclohexane) can be removed from the network by

sublimation (see Figure 2). Mostly, when speaking about freeze-drying, water will be the solvent. Although identical from a physical point of view, the same procedure for organic solvents is called "organic solvent sublimation drying" (OSSD).[7-9] In this, no capillary forces occur and the network will be retained. However, the freezing procedure may cause some damage to the gel network, hence, not fully keeping the initial structure intact.

## Supercritical drying the key to aerogels

The least invasive drying procedure is the supercritical drying (see Figure 2). For this method the liquid in the initial solvogel needs to be replaced by a solvent whose critical point is within a moderate temperature and pressure range, so that the network material does not degrade and the conditions can be achieved with standard technical apparatus. Increasing the temperature and the pressure beyond the critical point leads to a transition from the liquid phase to a supercritical fluid without crossing a phase boundary. This is very important for the retention of the gel network because thereby no capillary or crystallization forces will occur. Finally the pressure is reduces while maintaining a constant temperature und the supercritical fluid transforms into a gas, again without crossing a phase boundary. Now the liquid in the three-dimensional network is completely substituted by a gas and hence an aerogel is obtained.

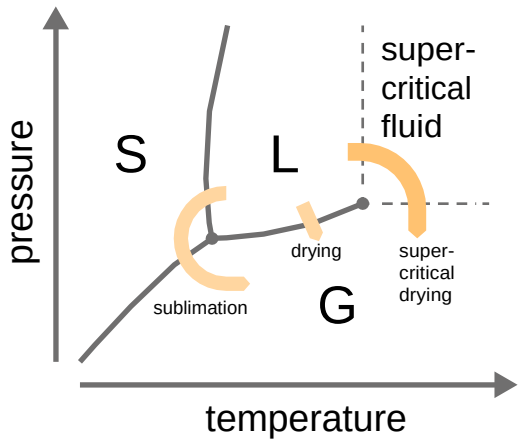


**Figure 2.** Phase diagram of the liquid phase to be removed from the gel network. Simple drying is the direct transition from the liquid to the gaseous state. In freeze-drying or OSSD the liquid is first cooled to the solid state and then under decreased pressure transformed into a gas via sublimation. Heating the liquid under elevated pressure brings it to the supercritical state. Lowering the pressure under constant temperature results in the gaseous state. In this transition from the liquid to the gas phase no phase boundaries are crossed.

Many groups from different areas have been investigating aerogels and the mechanism of gel formation, realizing more material combinations and more applications. Especially the oxide-based materials, which are accessible via the classical gelation route, have been studied in great detail. Several comprehensive reviews cover the most important work on the classical field of aerogels.[3-5] In this work we will focus on stable colloidal solutions as the starting material for aerogels and not on molecular precursors.

## Embedding nanoparticles into gels

A big disadvantage of classical gel formation is its limitation to only certain materials that can be obtained as a gel. Many optical and electronic properties of nanostructures, however, will depend on the precise control of the size, shape and composition. Nanoparticles from colloidal synthesis usually show their special properties only as long as they are well dispersed. For pure optical applications like color converters and luminescent solar concentrators it is sufficient to embed the nanoparticles into a transparent solid like polymers, glasses or salts.[10-15] However, if an additional accessibility of the individual nanoparticles is still needed, as for instance in photocatalysis, an immobilization of the nanoparticles onto a porous scaffold material is desirable. As a transition between classical aerogels and the recently emerged aerogels obtained through the controlled destabilization of pre-formed nanoparticles there are several reports on the embedding of different kinds of nanoparticles into aerogels for various applications.

The group of Rolison reported the incorporation of pre-formed Au colloids with different nanoparticle sizes into a silica aerogel matrix while preserving the plasmonic properties of the individual nanoparticles.[16] Later they could extend this work to many different types of nanoparticles (see Figure 3).[17] These composite materials combine the macroscopic properties of the silica gel and the individual properties of the nanoparticles used.

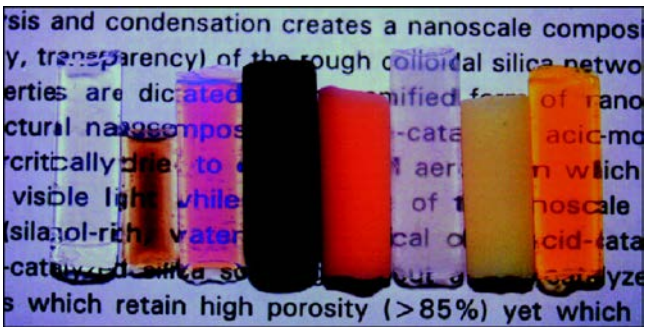


**Figure 3.** Silica-based composite aerogels (from left to right): pure silica aerogel; colloidal Pt– silica composite aerogel (2- to 3-nm Pt sol); colloidal Au–silica composite aerogel (30-nm Au sol); carbon black–silica aerogel (Vulcan carbon black, XC-72); FeII(bpy)3NaY zeolite–silica composite aerogel (0.1- to 1-μm zeolite crystallites); titania (aerogel)–silica composite aerogel (micrometer-size particulates composed of ~15-nm TiO2 aerogel domains); titania-silica composite aerogel (20- to 40-nm Degussa P-25 TiO2); and poly(methylmethacrylate)-silica composite aerogel (polymer $M_W \approx 15{,}000$, sieved to <44 μm).

The optical transparency of silica aerogels makes them an ideal host to increase the applicability for luminescent materials. Several reports show this for many different emitters like dyes,[18] CdSe/ZnS core/shell quantum dots,[19,20] carbon quantum dots,[21] nanodiamonds with nitrogen vacancies,[22] and silicon nanocrystals.[23] In all these examples the optical properties of the nanoparticles can be preserved in the macroscopic material.

This embedding strategy is not limited to silica aerogels material but has been shown for other host materials like cellulose,[24] agarose,[25] titania[26] and several others.

## Changing the way - leaving classical gelation behind

In 2005 Stephanie Brock with her work on the controlled destabilization of semiconductor nanoparticle colloids to form semiconductor aerogels revolutionized this field.[27,28] Therein the destabilization is initiated by the chemical oxidation of the thiolate surface capping groups. This leads to a controlled aggregation and network formation of the initial nanoparticles. The final aerogels can be obtained through supercritical drying. Interestingly, the aerogels obtained still show quantum confined optical properties.

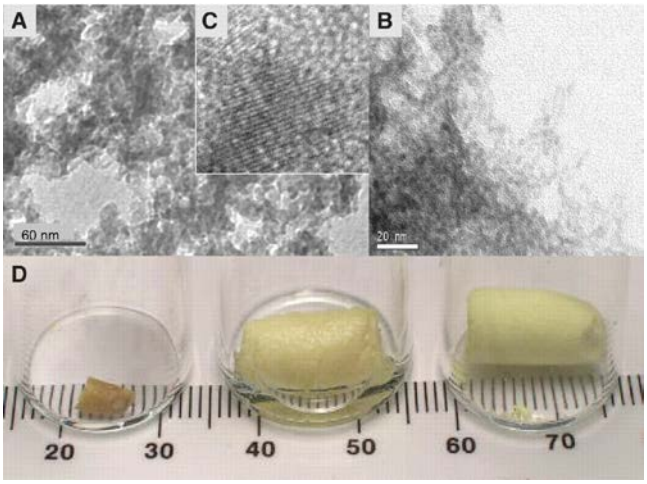


**Figure 4.** Different cadmiumchalcogenide gels made from pre-formed stable colloids.

But why was this step so important? Starting from stable colloidal solutions allows for the precise tuning of the starting material. For example the luminescent properties of quantum dots can easily be adjusted by controlling their size, plasmonic properties of metal nanoparticles strongly depend on shape, size and composition and even the catalytic activity of materials can be tuned by preparing nanoparticles with certain composition and facets.Lit In general, the mostly inorganic material of the core of nanoparticles determines its physical properties. The mostly organic shell, however, is responsible for the stability of the colloidal solution. For most applications the big challenge is to arrange the nanoparticles into macroscopic structures while still preserving their unique properties. Brock and coworkers approach introduced a new possibility to achieve this goal by destabilizing the nanoparticles in a controlled manner and hence arranging them into a three-dimensional gel structure.

For a controlled destabilization it is important to know how the initial particles are stabilized. The destabilization strategy to form gel networks from stable colloidal solutions will strongly depend on the kind of the nanoparticles stabilizer. Charge stabilization and stearic stabilization are the most common forms. In polar solvents nanoparticles can be charge stabilized. Their zeta potential, the effective outside charge, is usually above 30 meV or

below -30 meV for positively and negatively charged particles, respectively. Particles that come close to each other will repel because of electrostatic interactions. Hence, an agglomeration is prevented. Decreasing the magnitude of the zeta potential will destabilize the sol. If the concentration and rate of destabilization is within a certain regime this will lead to a network formation. The most common organic stabilizers used in colloidal synthesis are sodium citrate, mercaptopropionic acid (MPA), thioglycolic acid (TGA) and 5-mercaptomethyl tetrazole. Recently, also inorganic ligands like halogen ions, transition metal complexes and metal chalcogenide clusters found applications as electrostatic stabilizers.

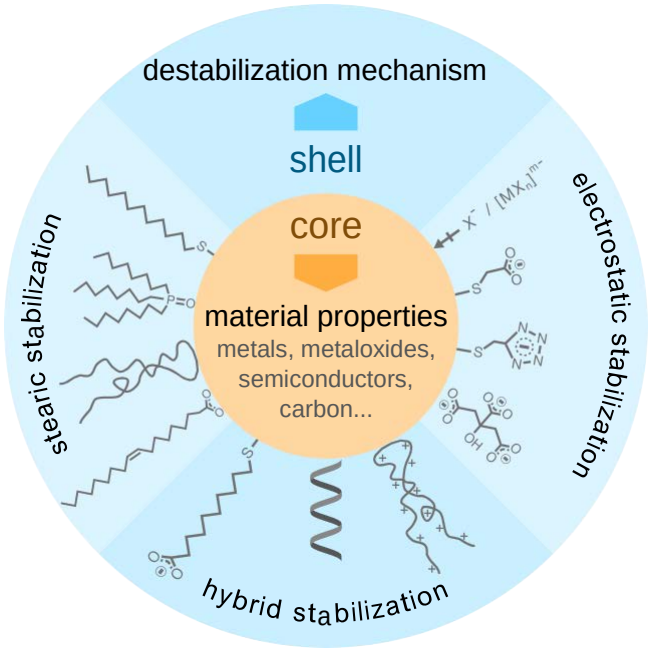


**Figure 5.** Overview of most common stabilizer types for colloidal nanoparticles. With respect to the final gels obtained from pre-formed nanoparticles the destabilization procedure usually depends on the kind of stabilizer present on the nanoparticle surface. The core material will mainly determine the material properties of the gel.

Especially in nonpolar solvents, nanoparticles are stabilized sterically. Here a shell of organic molecules surrounding each nanoparticle prevents touching of the surfaces and a subsequent agglomeration. Removing a part of the molecules in the shell will slightly destabilize the particles and a network formation is possible. When the stabilizers are strongly bound to the surface of the nanoparticles, as e.g. for thiols, they can be removed by a chemical or a photochemical oxidation. Washing or dialyzing the colloidal solution may remove loosely bound stabilizers, like polymers, and enable a controlled destabilization. Some prominent stearic stabilizers used in nanoparticle synthesis are trioctylphosphine (TOP), trioctylphosphine oxide (TOPO), oleic acid (OA), oleylamine (OAm), 1-dodecanthiol (DDT) and polymers like polyvinyl alcohol (PVA) or polyvinylpyrrolidone (PVP). Of cause, there are also hybrid stabilizers like mercaptoundecanoic acid (MUA), thiolated single stranded DNA (ssDNA) and polydiallyldimethylammonium chlorid (PDDA).

So far people refer to aerogels as materials derived from the classical sol-gel process. In the past decade a development of separating sol and gel step led to far more possibilities. A stable sol, a solution of any kind of nanoparticle in means of shape and material is the starting point. With this the properties of the nanostructures are controllable which is the great advantage of this strategy. The gel-formation step is separated. This gives additional control over the final morphology. Indeed, usually the formation of the gel is not a classical gelation but rather a flocculation. Which means, the gel is not necessarily filling the whole volume and the physical properties do not cross a gel point. The final step to form the aerogel is comparable to the classical removal of the liquid from the pores. Most commonly supercritical drying is used to prevent strong capillary forces to break the fine pore structure during solvent removal.

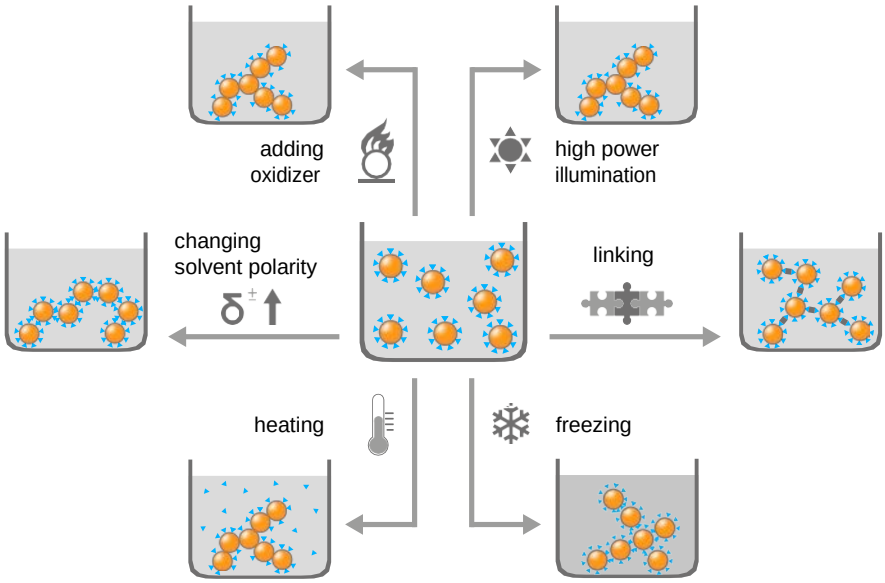


**Figure 6.** Strategies for the controlled destabilization of pre-formed colloidal solutions. This does not follow the classical gelation approach but is rather a flocculation. Triggered by different stimuli gel structures can be obtained. irgendwo noch washing

Depending on the stabilizer of the initial nanoparticles different destabilization strategies were developed during the past decade. One approach is to remove the ligands from the surface of the nanoparticles by chemical or photochemical oxidation (see Figure 6). Besides it is possible to remove loosely bound ligands by either washing or heating the respective sol. A general approach, which is independent from the stabilizer, is the freeze-gelation or ice-templating. Here the network formation of the dispersed particles is induced by the solidification of the solvent. A change in the polarity of the solvent can also induce a slow destabilization of the colloidal solution. Finally, the functionality of the ligands can be used to link the particles together and hence form a gel network.

## Gels from metal nanoparticles

For many chemical and catalytic application metals are very attractive materials. Especially in heterogeneous processes a high surface to volume ratio is desirable, which can be found porous metal materials. Dealloying is a widespread approach to porous metals. For this, an alloy of two metals with significantly different redox potential is formed. The non-noble metal can be dissolved chemically or electrochemically and the remaining noble metal forms a porous framework.[29-32] As an innovative method to obtain porous metals the Leventis group introduced the so-called nanosmelting. In this, a heat induced redox reaction between interpenetrating networks of resorcinol-formaldehyde and iron oxide aerogels result in ferromagnetic and superparamagnetic porous pig iron.[33-35] Besides, there are several reports on combustion and pyrolysis synthesis approaches to yield nanoporous metal foams.[36] A pure electrochemical access to porous metals has also been reported.[37-39] Here, a porous metal film is deposited under high current densities. This leads to a diffusion-limited growth of dendritic structures that can further be templated by evolving hydrogen bubbles. Since these materials are electrical conductive throughout the network they are very promising for applications as electrode materials with a large surface area and fast diffusion rates.

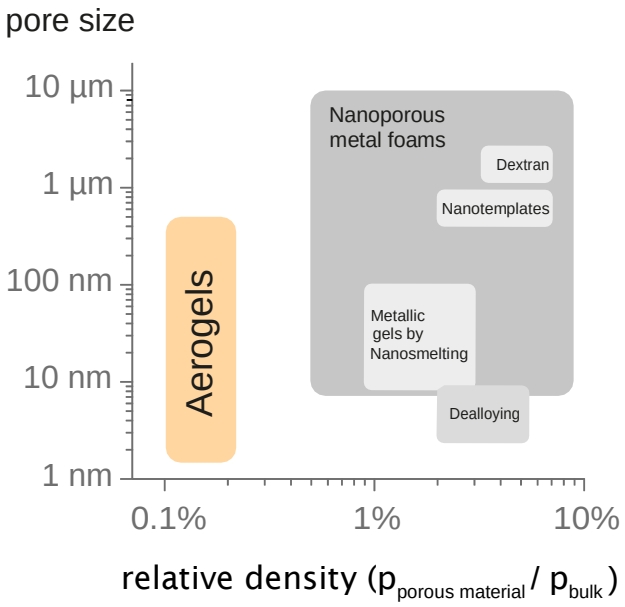


**Figure 7.** Relative density/pore size parameter space. Adapted from ref.[40]

In 2009 the Eychmüller group realized the synthesis of the first noble metal aerogels.[41] These gels show very low densities compared to the bulk material and their network structure exhibits much smaller features than other porous metal materials (see Figure 7). Starting with citrate stabilized gold, platinum and silver particles the concentration of the particles was increased with the help of membrane filters and subsequently the washed and concentrated

colloids were destabilized in a controlled manner by changing the solvent polarity or by adding an oxidizing agent. Finally, these hydrogels were dried in supercritical $CO_2$ to obtain the metal aerogels. The resulting black monoliths are made of an extremely fine sponge-like network (see Figure 8).

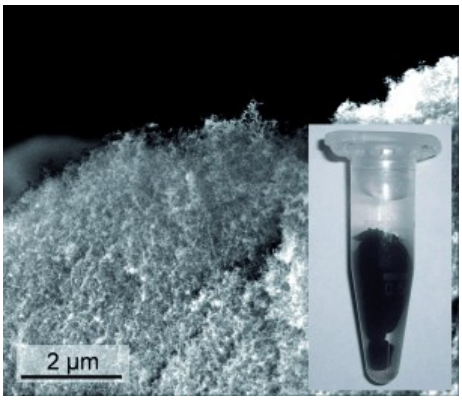


**Figure 8.** Noble metal self-supporting aerogels. The black monoliths (inset) consist of en extremely fine network of interconnected nanoparticles.[41]

In this, retention of the nano sized features could be observed since the diameter of the wires building the network is comparable to the size of the initial metal nanoparticles. Compared to other porous metal materials aerogels have extremely low densities and therefore occupy a new area in the pore size versus relative density parameter space (see Figure 7). Besides, among all porous metal materials noble metal aerogels exhibit record high specific surface areas when expressed in $m^2/mol$.[40]

Further studies of the co-gelation of different metal nanoparticles showed different element distribution patterns in the final aerogels depending on the metal combinations (see Figure 9).[40,42]

Elemental composition determines spatial elemental distribution

From EDX mapping studies it was found that a combination of initially pure Au and Ag nanoparticles results in an alloy of the two metals in the final aerogel. It is well known that these metals are likely to form alloys in the nano particulate state.[43] More surprisingly, the elemental distribution is different in the final gels made of combinations of Au-Pd and Pt-Pd, respectively. In Pt-Pd aerogels the scaffold backbone is mainly made of Pd decorated with Pt nanoparticle clusters. No alloy formation was observed for this material combination, which is also not to be expected, since the two metals do not form alloys at room temperature. The

most interesting spatial elemental distribution was found in the Au-Pd system. Here individual Au nanoparticles are embedded in the Pd scaffold. In other words, the formerly individual Au and Pd nanoparticles form Au/Pd core/shell particles that build up the aerogel network in a necklace like manner. These structures could be very interesting for photocatalytic applications. Since the Pd is less noble than Au a selective reduction would result in Au nanoparticles that are embedded in an oxidic matrix. Similar structures have recently shown great potential as photocatalysts using hot electrons to enhance gas phase reactions.[44]

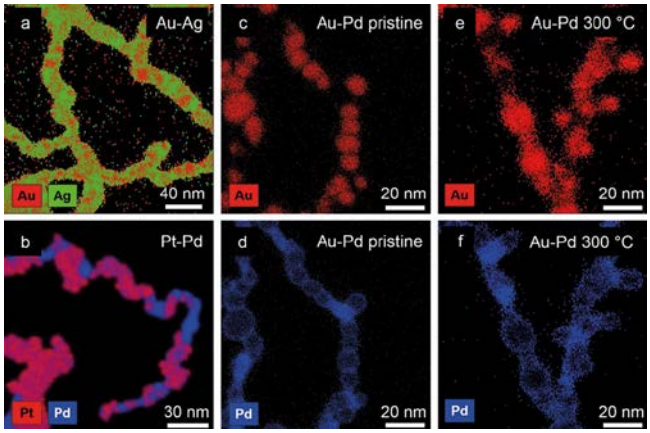


**Figure 9.** Elemental EDX maps of several bimetallic aerogel samples with an initial atomic ration of 1:1. Au/Ag aerogels are made of a network that consists of an alloy of the two metals. In Pt/Pd aerogels the metals separate along the network and form islands, whereas the Pd is forming the backbone. A core/shell structure can be found in the Au/Pd aerogels. Here the Au/Pd core/shell structures form a necklace-like network.[42]

Not only spherical metal nanoparticles can be used as a starting material for metal aerogels. Using the freeze gelation approach and subsequent freeze-drying a stable suspension of copper nanowires could be transformed into a copper aerogel.[45] The density and the mechanical properties of the final gels are adjustable by changing the initial nanowire concentration. Furthermore, after a surface modification these materials can be used as selective absorbents of organic solvents. Using the ice-templating approach cryogels from silver nanowires can also be formed.[46] These show a 3D binary-network architecture und very promising electromechanical properties. Alternatively, copper nanowire aero- or rather cryogels have been obtained from pre-formed hydrogels via freeze-drying.[47] The hydrogels are formed in a one step approach during the solvothermal synthesis of the nanowires itself. Changing the initial precursor concentration enables the control of the density, porosity, electrical, thermal and mechanical properties. Especially the thermal conductivity of this material makes it very promising for applications as heat sinks.

The freeze gelation approach was recently extended to numerous different starting materials. In this, it was possible to obtain Au, Ag, Pd and Pt cryogels from stable colloids of the respective metals.[48] Furthermore, cryogelation enables the control of the final macroscopic

shape of the gel through casting the colloid in a specific mold prior to gelation. Nanoscopic properties of the initial particles, like localized surface plasmons, could partially be retained (see Figure 10).


**Figure 10.** A) Photographs of aerogels of Au, Ag, Pd, Pt, Fe2O3, and CdSe/CdS rod-like NPs (scale bar: 1 cm). B) Influence of NP volume fraction of the colloidal solution on the final volume of the monolith, both resulting from 1 mL Pd-colloid (volume fractions of $2.5 \times 10^{-4}$ % and 0.25 % from left to right, respectively). C) Examples for a variety of shapes possible by cryogelation route: smiley in a Petri dish or thin film on glass slide.[48]

Metallic aerogels could also be formed through the destabilization of metal nanoshells.[49-52] In this, the initial nanoshells are produced via a galvanic replacement reaction of initial Ag and Ni nanoparticles, respectively. Au/Ag, Pd/Ag and Pt/Ag alloyed nanoshells were first concentrated by either simple solvent evaporation or with the help of centrifuge membrane filters. Colloidal solutions concentrated through solvent evaporation spontaneously formed a gel when stored in the dark for several days, whereas the nanoshell solution concentrated with centrifuge filters could be destabilized by the addition of NaCl.[49] Pd/Ni alloyed nanoshells colloids where also concentrated with the help of centrifuge filters first. The gelation, however, was induced by heating the colloid at 75 °C for six hours.[50] Pure Ag nanoshells could be assembled into opaque and transparent gels by first concentrating the colloid followed by the oxidation of the surface ligands. The etching of the nanoshells into significantly smaller nanoparticles is responsible for the formation of the transparent gels.[51] Self-supporting Au/Ag aerogels made from tunable Au/Ag nanoshells through the oxidative removal of surface ligands have been successfully investigated as surface-enhanced Raman scattering (SERS) substrates.[52] A 20-fold increase in SERS intensity was achieved in the final gels compared to the initial nanoparticles.

Mainly, metal aerogels are prepared by the subsequent nanoparticle formation and concentration followed by one of the controlled destabilization procedures. However, it is also possible to obtain metal aerogels from a one step approach where the particles are formed and directly start to aggregate into three-dimensional gel like structures (see Figure 11). In general, this approach resembles to some extend the classical gelation approach. Starting from a molecular precursor in solution, which will be transformed into a sol by reduction, the final gel is build by the interconnection of the not stabilized metal nanoparticles formed.[53,54]

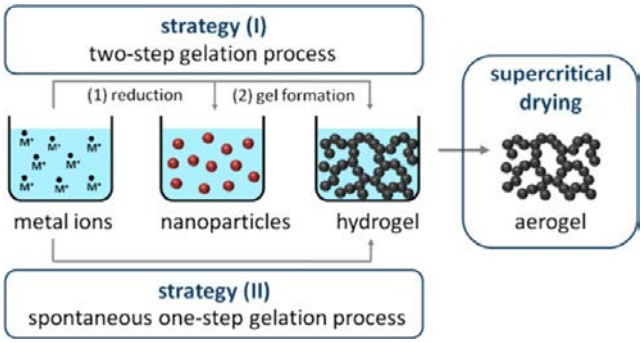


**Figure 11.** Gel formation strategies for noble metal nanoparticle gels.

Metal nanoparticles especially noble metal nanoparticles are very prominent candidates for catalysts. In real applications they are usually immobilized on a porous scaffold that could either be inert or an active partner in the reaction catalyzed. With these classical materials there have been always problems like obtaining uniform particle sizes, equal distribution on the host and to achieve a strong binding to ensure that the particles are not removed during the application. As a new emerging class of materials with high specific surface areas and large open pores, metal aerogels with metal backbones are very promising in various applications such as in heterogeneous gas phase catalysis, electrocatalysis, sensors, and energetic materials.[55]

Metal aerogels
a giant leap
for electrocatalysis

The sluggish kinetics of the oxygen reduction reaction (ORR) and alcohol oxidation, insufficient catalyst stability and high cost are among the most important obstacles for the widespread use of fuel cells.[56] Increasing research efforts are therefore being carried out to develop facile methods and design more efficient cathode and anode electrocatalysts with

long-term durability. Metal aerogels combine several beneficial properties making them superior to other materials for electrocatalysis. The special pore structure spanning multiple orders of magnitude allows for a fast material transfer while at the same time offering a large specific surface area. The interconnected backbone ensures an electrical conductivity throughout the whole network. Besides self-supporting character of the aerogel eliminates the problem of loosing the noble metal nanoparticles in catalysis due to a weak metal-support interaction. Last but not least, the constituting elements in the multimetallic aerogels can be well controlled, which facilitate the fully exploitation of the synergistic effects in enhancing the catalytic activity. In the following part, we will discuss the progresses of application of metal aerogels as electrocatalysts for anode and cathode reactions of fuel cells.

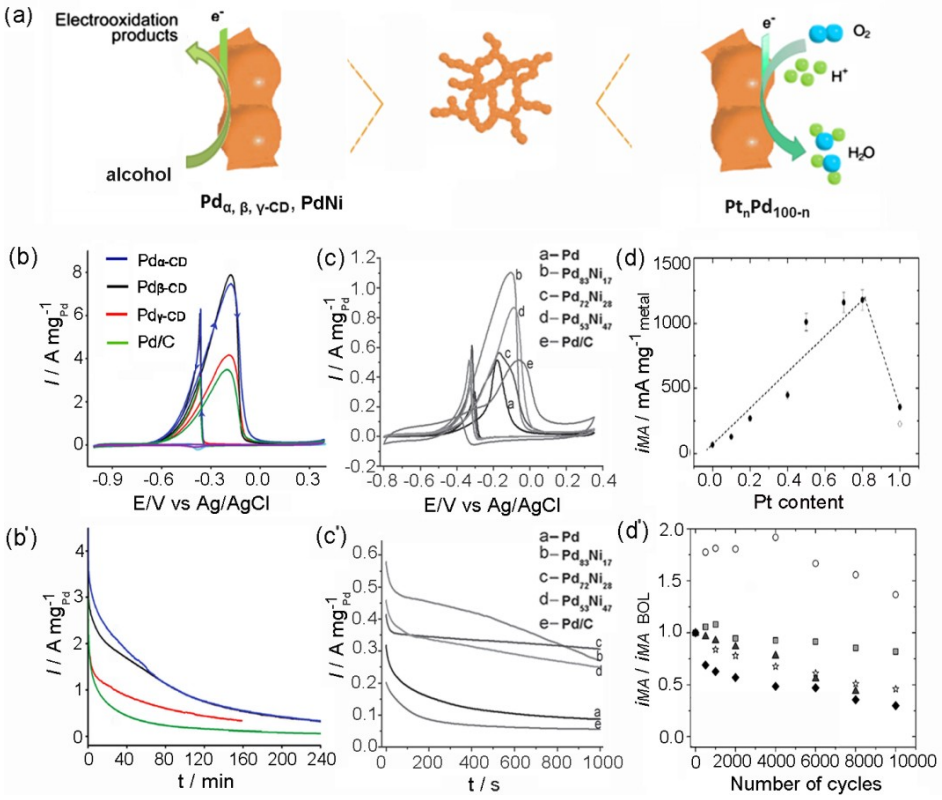


**Figure 12.** (a) Schematic illustration of electrocatalytic activities of $Pd_{\alpha,\ \beta,\ or\ \gamma\text{-}CD}$ and PdNi aerogels toward alcohol (ethanol, methanol) oxidation and $Pt_nPd_{100-n}$ aerogels toward the ORR. (b) Cyclic voltammograms of electrodes modified with $Pd_{\alpha,\ \beta,\ or\ \gamma\text{-}CD}$ aerogels and Pd/C in 1.0 M KOH + 1.0 M $C_2H_5OH$ aqueous solution. (b') Chronoamperometric curves for ethanol electrooxidation at -0.3 V. (c) CVs of PdNi with different compositions, Pd and commercial Pd/C electrodes in aqueous 1 M KOH + 1 M methanol solution at a scan rate of 50 mV/s. (c') Current density–time curves of PdNi with different compositions, Pd and commercial Pd/C electrodes in aqueous 1 M KOH+1 M methanol solution at –0.2 V. (d) Volcano plot of the ORR mass activity of various $Pt_nPd_{100-n}$ aerogel catalysts as a function of Pt content at 0.9 V/RHE. The empty circle represents the value for Pt/C. (d') Relative ORR mass activity of various $Pt_nPd_{100-n}$ catalysts as a function of the number of potential cycles (linear potential sweeps between 0.5 and 1.0 V/RHE). ○ $Pt_{40}Pd_{60}$, ■ $Pt_{80}Pd_{20}$, ▲ Pt, ◆ Pd, ☆ 20% Pt/C. (a-e) reproduced with permission from ref. [53,54], copyright 2012, 2013 WILEY-VCH Verlag GmbH & Co. KGaA, Weinheim.

The Eychmüller group synthesized cyclodextrin protected Pd ($Pd_{\alpha,\ \beta,\ or\ \gamma\text{-}CD}$),[53] pure $Pt_nPd_{100-n}$,[54] Au,[57] and PdNi[50,58] aerogels and studied their electrocatalytic potential.[55] The

electrocatalytic performances of the $Pd_{CD}$ aerogels were evaluated by cyclic voltammetry and chronoamperometry and compared to the commercial Pd/C (10 wt%).[53] Herein, $Pd_{CD}$ aerogels show much higher mass-specific current densities in the forward scan toward ethanol oxidation, enhanced kinetics, slower current decays and higher steady-state current densities (see Figure 12).

The PdNi ($Pd_{83}Ni_{17}$, $Pd_{72}Ni_{28}$ and $Pd_{53}Ni_{47}$) bimetallic aerogels were investigated toward methanol oxidation and compared with the Pd aerogel and commercial Pd/C (see Figure 12).[58] Among the three PdNi aerogels, $Pd_{83}Ni_{17}$ possessed the highest activity and displayed a less positive anodic onset potential and the highest mass current density. In comparison with the Pd aerogel and the Pd/C, the optimized $Pd_{83}Ni_{17}$ afforded the preeminent electrocatalytic activity with higher current density, suggesting the crucial role of the Ni in the electrocatalysis. The chronoamperometry tests show that all the PdNi aerogels exhibit much higher initial polarization mass-specific current densities and higher steady-state current densities for the methanol electrooxidation than the Pd aerogel and the Pd/C, indicating the higher electrocatalytic activity and durability of the PdNi aerogels.

Monometallic and bimetallic $Pt_nPd_{100-n}$ aerogels have been evaluated and compared with Pt/C (20 wt%) for the ORR investigations (see Figure 12).[54] The specific activity (based on the total metal loading) at 0.9 V as a function of Pt content in the aerogels shows a Volcano-type behavior with the $Pt_{80}Pd_{20}$ aerogel exhibiting the highest mass-specific activity and being five times higher than the commercial Pt/C catalyst. The downshift of the d-band center in the alloys, commonly used as a descriptor of the surface electronic state of ORR catalysts, shows the same volcano-type behavior for the $Pt_nPd_{100-n}$ aerogels.[59-63] The prominent activity of the $Pt_{80}Pd_{20}$ aerogel indicates the best balance between the free energies of adsorption of oxygen-containing reaction species. Durability test results indicate that the bimetallic aerogels show much better durability than the pure Pt and Pd aerogels as well as Pt/C.

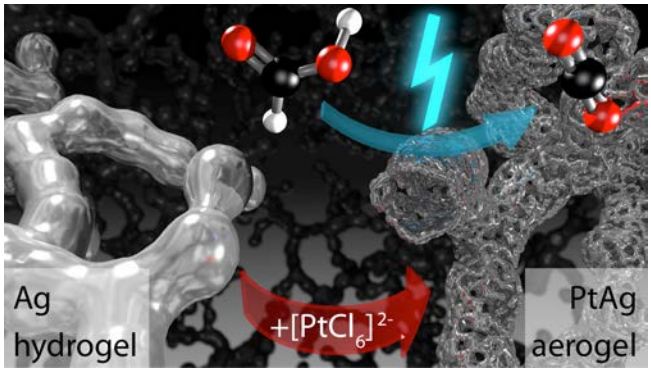


**Figure 13.** Nanotubular Pt/Ag aerogels obtained through the galvanic displacement reaction from Ag hydrogels.[64]

Another interesting approach towards highly efficient electrocatalysts is the formation of hollow gel structures from pre-formed solid gel networks through galvanic replacement. Following this strategy PtAg alloy nanotubular aerogels with hierarchical porosity could be obtained from Ag hydrogels (see Figure 13).[64] In formic acid electrooxidation, the metal-based mass current density of the final gels is 19 times higher than commercial Pt black. Except this superior electrocatalytic activity, the material shows an outstanding electrochemical and structural durability.

The excellent electrocatalytic activity and durability of the $Pd_{CDs}$, the PdNi, the $Pt_nPd_{100-n}$ and the PtAg nanotubular aerogels discussed above suggest that unsupported noble metal based aerogels can be considered as a new class of very promising fuel cell electrocatalysts which combine the high stability of extended surfaces with the high surface area of nanoparticles. Not only the large surface area and high porosity of these aerogels play a great role in their electrocatalytic properties, but also the left stabilizers on the aerogel surfaces and synergistic effects of different metal constituents have great influence on their electrocatalytic performances.

## Metal aerogels for bioelectrocatalysis

Besides the excellent performances of metal aerogels in the areas discussed above, they also have outstanding performances in bioelectrocatalytic applications and biofuel cells due to their high porosity, large surface area, and excellent catalytic activity. The bioelectrocatalytic application of Pd aerogels (generated by destabilizing colloidal solutions of citrate stabilized Pd nanoparticles with various concentrations of calcium ions) as electrode enhancing materials was demonstrated by constructing an integrated Pd aerogel-based enzyme (such as glucose oxidase (GOD)) electrode and investigating their activities toward ferrocene (FC)-mediated glucose oxidation.[65] Compared with the responses of GOD-Nafion and Pd NPs-GOD-Nafion, the Pd aerogels show overall much faster electron-transfer kinetics of the mediator FC at the Pd aerogel-based enzyme film surface. In the presence of glucose, the Pd A-GOD-Nafion/GC exhibited much higher bioelectrocatalytic activities compared with the GOD-Nafion/GC and Pd NPs-GOD-Nafion/GC electrodes, indicating a dramatic increase in the bioelectrocatalytic function of the Pd aerogel modified electrodes. In addition, the Pd aerogel-based enzyme electrodes showed 12 h stability under continuous operation and ~95%

of catalytic current upon storage at 4 °C for 2 weeks. These electrochemical results show that the Pd aerogel-based enzyme electrodes exhibit high activities toward the FC-mediated oxidation of glucose, which could promise potential applications of the high-performance glucose biosensors and glucose/$O_2$ biofuel cells (BFCs).

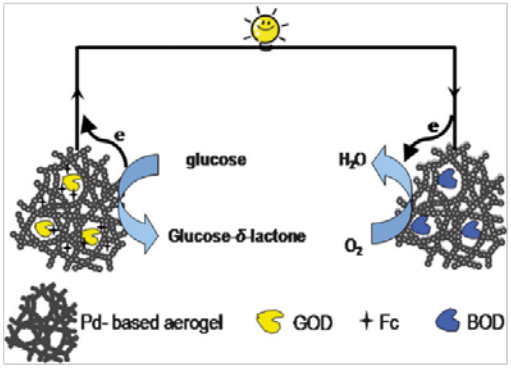


**Figure 14.** Schematic illustration of the working principle of the membraneless glucose/$O_2$ BFC based on Pd aerogels.[66]

Considerable research interest has been focused on enzymatic BFCs, among which the glucose/$O_2$ BFCs are envisaged to be able to power bioelectronics in vivo.[67-69] The commonly used enzymes for glucose oxidation generally need mediators or cofactors, and thus a separating membrane to avoid crossover reactions in the BFC system, which increases the cost and difficulty for miniaturization. To solve these issues, immobilizing enzymes together with mediators to form integrated bioelectrodes are demonstrated to be an effective way.[70-72]

The membraneless glucose/$O_2$ biofuel cell using Pd-based aerogels as electrode materials was generated (see Figure 14).[66] The bioanode consists of $Pd_{\beta\text{-CD}}$ aerogel with a coimmobilized mediator and glucose oxidase for the oxidation of glucose, in which ferrocenecarboxylic acid was integrated into the three-dimensional porous $Pd_{\beta\text{-CD}}$ aerogel to mediate the bioelectrocatalytic reaction. Bilirubin oxidase and $Pt_{75}Pd_{25}$ alloy aerogel were confined to an electrode surface, which realized the direct bioelectrocatalytic function for the reduction of $O_2$ to $H_2O$ with a synergetic effect at the biocathode. The glucose/$O_2$ biofuel cell assembled with these two bioelectrodes showed a maximum power output of 20 μW $cm^{-2}$ at 0.25 V. The work provides a novel method to construct a porous mediator system that supports the biocatalysts and enables the direct electrical contact between BOD and the aerogel-modified electrode.

## Gels from metal chalcogenide nanoparticles

Until the pioneering work from Brock there where no comparable porous metal chalcogenide materials available (see also chapter "Changing the way - leaving classical gelation behind"). State of the art were the just emerged chalcogenide zeolite analogs[73-75] and chalcogenide macroporous materials grown in photonic crystal templates.[73,76,77] Taking stable colloidal solutions of metal chalcogenides and assembling them into macroscopic structures, directly opened a new field of research. Especially the unique optical properties of quantum dots are very interesting.[78] Due to the confined dimension of quantum dots these become size dependent and can therefore be tuned easily. For applications, however, the nanoscale properties have to be transferred to the macroscale. One approach is the controlled assembly into super lattices.[79] In this, the particles order into regular arrangements that are analogue to atomic lattices. However, the individual particles are not accessible anymore and usually the superstructures are not conductive due to a layer of insulating stabilizers between the individual particles, making them hardly usable for electrical applications. Besides, because of the high density a significant reabsorption makes these superstructures not very promising for optical applications.

### Quantum confinement at the macroscopic level

Already within their first studies the Brock group could show quantum confined absorbance properties for different metal chalcogenide gels.[28,80,81] Furthermore they showed that the surface of the particles is still exposed and can be modified even after the assembly. In a later study this feature was used to extend the possible aerogel materials to PbSe and CuSe through a cation exchange reaction in the pre-formed CdSe gels.[82] Using CdSe/ZnS core/shell nanoparticles as base material they obtained the first self-supporting luminescent semiconductor aerogel (see Figure 15).[83] First the synthesized QDs were surface exchanged with MUA and transferred to methanol to yield highly luminescent colloids. The destabilization was induced by the addition of the oxidizing agent NMO. After an aging time of several days the final aerogels were obtained from supercritical drying. In contrast to the gels from pure CdSe nanoparticles the band edge emission of the CdSe/ZnS xero- and aerogels was well preserved and only slightly shifted compared to the nanoparticle sol. This

was mainly attributed to the protection of the CdSe cores by the ZnS shell, preventing the formation of trap states.

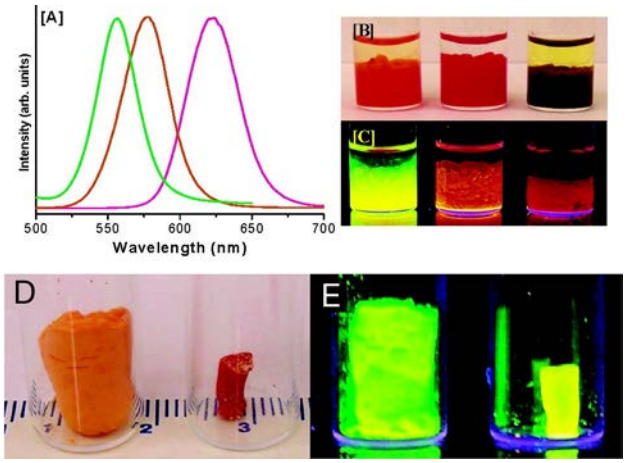


**Figure 15.** Preservation of the luminescent properties from quantum dots in macroscopic gels. The photoluminescent properties of the initial CdSe/ZnS sols could be retained in the gel structures. Solvogels under white light (B) and UV light (C); Aeorgels (left) and Xerogels (right) under white light (D) and UV light (E).[83]

In subsequent studies they produced aerogels from nanoparticles with different shapes and investigated their optical and mechanical properties.[84,85] For instance, aerogels made from CdSe nanorods showed a 25 times more intense luminescence than compared to aerogels obtained from CdSe nanoparticles. Furthermore, gel structures obtained from rods or branched nanoparticles show superior mechanical strength and porosity compared to gels from quantum dots. This is mainly attributed to the polymer-like structure of these materials. Changing the density of CdSe gels has been used to tune their optical band gap.[86] In this, one reason is the quantum confinement, which depends on the domain size in the final gels. However, a different behavior for aero- and xerogels was observed. These effects were explained by the additional dipole-dipole interactions in densely packed xerogels. This observation correlates also with change in fractality from mass-fractals for aerogels to surface-fractals in xerogels, obtained from SAXS investigations. A different study showed that the size of the aggregates in an CdSe gel can be controlled by the amount of oxidizing agent added, resulting in a control between transparent and opaque solvogels.[87] In this work they also investigated the kinetics of the gel formation and the fractal dimensions of the final gels using time resolved DLS and SAXS.

The first luminescent aerogel obtained from aqueous thiol-stabilized CdTe colloids were reported in 2008 by the Eychmüller group.[88] They investigated different destabilization procedures and found that a photochemical treatment was most suitable to retain a high luminescence in the final gels. Besides, the intermediate hydrogels could be infiltrated with a

polymer resulting in luminescent composites with arbitrary shape. Later this group could extend their work on luminescent CdTe aerogels with a new destabilization approach using elevated temperatures and a changed solvent polarity.[89] The aerogels obtained are made of long interconnected wires. These wires are made of an amorphous Cd/TGA complex embedding the CdTe nanocrystals, hence acting as a stabilizer and a separator at the same time. Adjusting the pH of washed MPA stabilized CdTe nanoparticles in water could also successfully be used as gel formation procedure.[90] The gels obtained still show strong photoluminescence. Besides it was possible to incorporate Au nanoparticles into the CdTe network.

## Tetrazole stabilizers for reversible gel formations

The first reversible gel formation of II-IV semiconductor nanoparticles was shown by the Brock group in 2010.[91] CdSe gels that were obtained via the addition of the oxidizing agent NMO could be redispersed with an excess of the stabilizer MUA and adjusting the pH or adding a reducing agent. The obtained sol could then be regelated with NMO after washing. During this cycle the surface of the CdSe nanoparticles is etched and therefore the particles become smaller with every iteration.

In the same year the Eychmüller group introduced a very innovative approach to aerogels made from aqueous nanoparticle colloids.[92] They used a new stabilizer with a tetrazole functional group exposed to the surrounding making the particles charge stabilized. Adding $Cd^{2+}$-ions to the sol resulted in the complexation of the tetrazole groups with the metal ions and hence induced the network formation (see Figure 16). Introducing a stronger complexing agent like EDTA it was possible to remove the $Cd^{2+}$-ions from the gel dissolved in separated nanoparticles again. In this, the very high luminescence of the initial particles (PL QY 60 %) could almost be recovered completely.

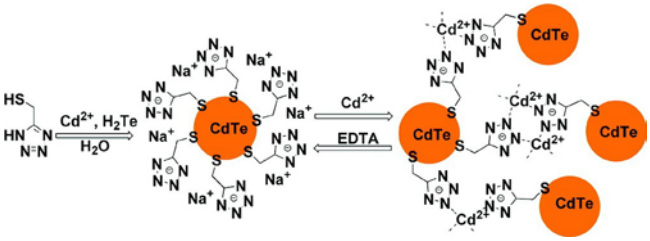


**Figure 16.** Reversible gel formation in tetrazole stabilized CdTe nanoparticles.[92]

In subsequent studies they successfully assembled a mixture of different quantum dots and quantum dots with a silica shell all stabilized with tetrazole ligands into aerogels.[93,94] For pure quantum dots assembled into gels they reported a change in the emission properties attributed to FRET (see Figure 17 left). This also proves that the network of the different quantum dots is randomly mixed and no separation was observed. Furthermore, by adjusting the ratios and emission wavelength of the initial particles they were able to prepare a white light emitting aerogel. Otherwise, using quantum dots with a silica shell for the gel formation the initial emission color remained unchanged. This is to be expected, since the particles in the final gel are still well separated by the silica shells, preventing an efficient FRET (see Figure 17 right).

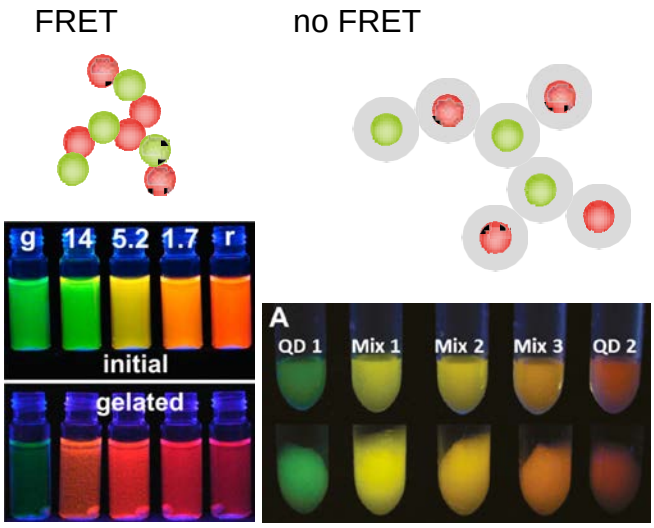


**Figure 17.** Assembling pure green and red emitting QDs results in a change of the emission color compared to the mixed colloids caused by an efficient energy transfer (left). In contrast, for quantum dots having a silica shell the emission color does not change during gelation (right).[93,94]

In 2011 the Kotov group reported a color switching behavior in reversible nanoparticle gels.[95] They extensively washed aqueous TGA stabilized CdTe nanocrystals and stored them for several month in the dark to induce the spontaneous network formation. Through sonication these loosely bound gels can be broken up into a nanoparticle sol again, accompanied by a change in the optical properties. In the same year the Brock group found that the gel formation induced by the oxidizing agent NMO could also be used for CdTe nanoparticles in organic solution.[96] By adding a reducing agent the gels obtained could reversibly be transformed back to the sol state.

Hydrogels and aerogels made from CdSe/CdS dot-in-rod nanoparticles were introduced by the Bigall group.[97] The nanorods where first transferred to the aqueous phase and then destabilized with the oxidizing agent $H_2O_2$. Finally the aerogels were obtained from

supercritical drying. These materials show very interesting optical properties. Compared to the nanorod sol the gel structures show up to four times longer fluoresence lifetimes. This can be explained by the interconnection of the CdS shells and the resulting delocalization of the electrons over a large part of the structure. The holes, however, will be localized to the CdSe cores that are evenly distributed among the gel structure. Furthermore, the photoluminescence quantum yield of the aerogels can retain or even exceed the values in the initial colloidal solutions.

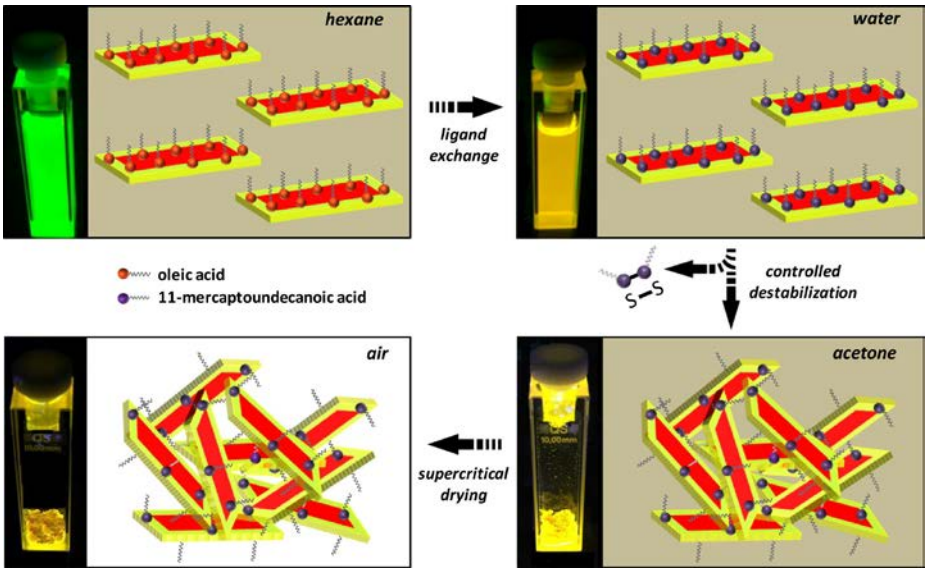


**Figure 18.** Luminescent aerogels from CdSe/CdS core/crown nanoplatelets.[98]

Just recently, the Bigall group successfully produced luminescent aerogels from colloidal quantum wells, also called nanoplatelets.[98] First they synthesized CdSe/CdS core/crown nanoplatelets, which were then transferred to aqueous solution. The destabilization was induced by the addition of hydrogen peroxide as an oxidizing agent to remove the thiolated stabilizers. Final aerogels were obtained through supercritical drying in $CO_2$. The two dimensional quantum wells have just the (111) facet exposed to the environment. This makes the nanoplatelet aerogels extremely interesting for selective sensing or catalysis studies. Besides, nanoplatelets show extraordinary optical properties like giant oscillator strength and almost no Auger-recombination. Retaining the luminescent properties of the nanoplatelets at the macroscopic level brings these materials closer towards applications.

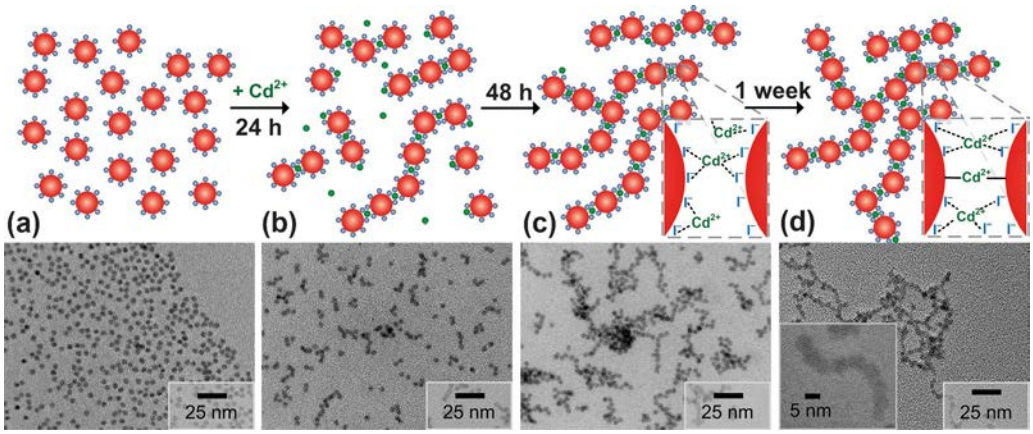


**Figure 19.** Gelformation of all-inorganic CdSe nanoparticles.[99]

Another very recent development is the production of gels from all-inorganic stabilized nanoparticles.[99,100] In this, the Eychmüller group used particles, where they exchanged the initial organic ligands to purely inorganic ones.[101] The resulting structures are especially interesting for electronic applications because the particles are not separated by bulky organic ligands, hence their conductivity is improved. Besides these materials are also promising candidates for catalytic applications because of their clean surfaces.

## Towards applications with semiconductor aerogels

Besides the significant amount of synthetic and characterization work, the Brock group investigated the usability of quantum dot gels in optoelectronic devices like solar cells.[102,103] Furthermore they show the preparation of transparent conductive films made of CdSe/ZnS core/shell nanoparticles obtained through a destabilization method.[104] The Eychmüller group showed the applicability of CdTe gels as biosensors.[105] For this, they immobilized an enzyme on the surface of the pre-formed gel. This composite material changed its fluorescence intensity upon the presence of an analyte because of an induced quenching mechanism.

Aerogels and solvogels from semiconductor materials are not just interesting for optical and electronic applications. A great potential of these materials is the role as adsorbents and heavy metal ion scavengers. Aerogels made of ZnS can clean water contaminated with $Pb^{2+}$, $Cd^{2+}$ and $Hg^{2+}$ through a cation exchange reaction binding the toxic metal ions and releasing the less toxic $Zn^{2+}$ ions into solution.[106]

Current approaches to improve the energy efficiency of heat loosing processes focus on the transformation of the heat loss into electrical energy with the help of thermoelectric materials. Here aerogels are also very promising candidates, because of their heat insulating and low thermal conductivity. The Brock group investigated PbTe and $Bi_2Te_3$ aerogels and found low thermal conductivities due to pronounced phonon scattering.[107,108] The gel network is produced from pre-formed colloidal solutions of the respective nanoparticles through an oxidative removal of the surface ligands. However, obtaining a high electrical conductivity in the final structures still is a challenge. If this can be overcome, these materials should show very high figures of merit.

Last but not least, another approach to metal chalcogenide aerogels was introduced and investigated mainly by the Kanatzidis group in parallel to the above-mentioned developments in semiconductor aerogels. So called chalcogels are produced by interlinking chalcogenide clusters with metal ions in aqueous solution.[109-111] Mechanistically, this method is comparable to the classical gel formation mechanism since the clusters used have a molecular size and form a polymer-like network. Chalcogels show very promising properties towards their use as catalysts,[112] in selective gas separation,[113] and for the removal of heavy metal ions and radioactive iodide from waste water, respectively.[114-118]

## Gels from oxide nanoparticles

Metal oxides are among the most studied materials in aerogel research. Most of the approaches reported to date follow the classical gelation mechanism and are summarized elsewhere.[3-5,119-121] Special attention aroused the work by Baumann and colleagues, wherein they introduced propylene oxide as an efficient reactant to obtain metal oxide gels without the need for the commonly used toxic and expensive alkoxide precursors.[122] This method was extended to several metal oxide systems like $Al_2O_3$, $CeO_2$, ZnO, $SnO_2$, $TiO_2$, $SiO_2$, $NiO_2$, $Fe_2O_3$ and others.[7,123-126] Current research in the field of the classical gelation approach to metal oxide aerogels focuses on the improvement of the electrical,[127,128] thermal,[129] and mechanical properties.[130] Especially the Leventis group made strong contributions to the field of oxidic aerogels by changing and improving their mechanical properties.[131-133]

Other than starting from molecular precursors or colloidal solutions of oxide nanoparticles there are also alternative ways to obtain aerogels not following the classical gelation route. Hollow nanotube aerogels have for instance been prepared by atomic layer deposition of $TiO_2$, ZnO and $Al_2O_3$ on a nanocellulose aerogel template, which could be removed afterwards through calcination.[134]

**Figure 20.** ATO aerogel obtained from destabilization of antimoni doped tinoxide particles after heat treatment.[135]

Because most of the metal oxides are available as aerogels through the classical gelation procedure, not much attention has been attributed to the destabilization of pre-formed metal oxide nanoparticles to obtain aerogels. Especially the Niederberger group pioneered this field with the successful production of several oxidic materials formed by the controlled destabilization of metal oxide nanoparticles. In a first proof of concept work they showed a co-gelation of pre-formed silica and anatase nanoparticles.[136] A mixture of trizma functionalized $TiO_2$ nanoparticles in water and silica nanoparticles in ethanol is heated at 60 °C for half an hour to induce the gelation. The final gels were obtained from supercritical drying. In a subsequent work they showed the gelation of pre-formed $BaTiO_3$ nanoparticles.[137] First they produced a stable sol of the particles in ethanol that could be

destabilized by changing the solvent polarity through the addition of water. The final monolithic gel can be transformed to an aerogel by supercritical drying. $BaTiO_3$ is an attractive material due to its superior piezo-, pyro- and ferroelectric properties.

Furthermore, they could extend their thermally induced gelation approach to antimony doped tin oxide aerogels.[135,138] The electrical conductivity of the final gels can be significantly improved adjusting the antimony content and applying postsynthetic treatments like annealing and UV curing. Electrically conductive oxide aerogels are very promising materials for applications in electrocatalysis and as battery, solar- and fuel-cell materials.

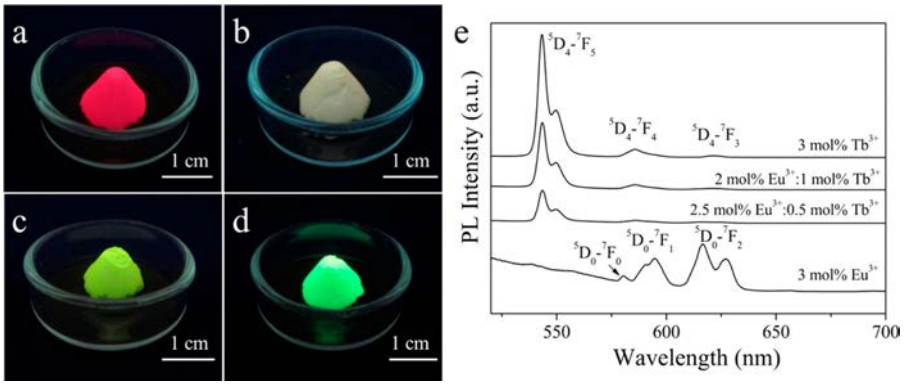


**Figure 21.** Rare earth metal doped $Y_2O_3$ aerogels.[139]

Just recently, the Niederberger group presented the formation of $Y_2O_3$ aerogels.[139] The gels were obtained from pre-formed $Y_2O_3$ nanosheets through a centrifugation-induced gelation process. Doping of the initial nanosheets with rare earth metals results in luminescent aerogels (see Figure 22). Besides the interesting optical properties these aerogels show a superior capacity for the adsorptive removal of methylene blue from aqueous solutions. These multifunctional gels are very promising for applications in optoelectronics, catalysis and wastewater treatment.

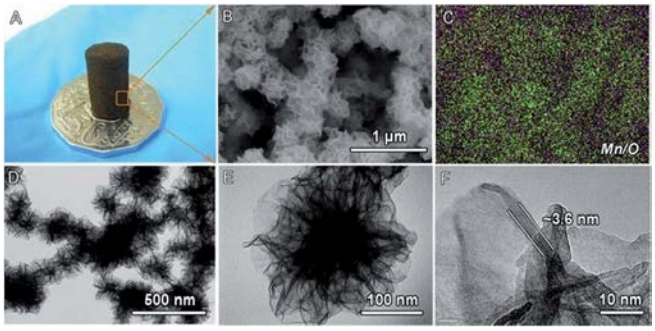


**Figure 22.** Hierarchical aerogel from $MnO_2$ nanosheets as starting material.[140]

Also starting from a stable nanosheet dispersion, $MnO_2$ aerogels can be obtained through freeze-gelation and subsequent freeze-drying.[140,141] The final materials are efficient absorbents to remove toxic vapors from air.[141] Besides the hierarchically structured $MnO_2$

aerogels can be used as electrodes in Li-$O_2$ batteries and a great potential as catalysts for the ORR and OER.[140]

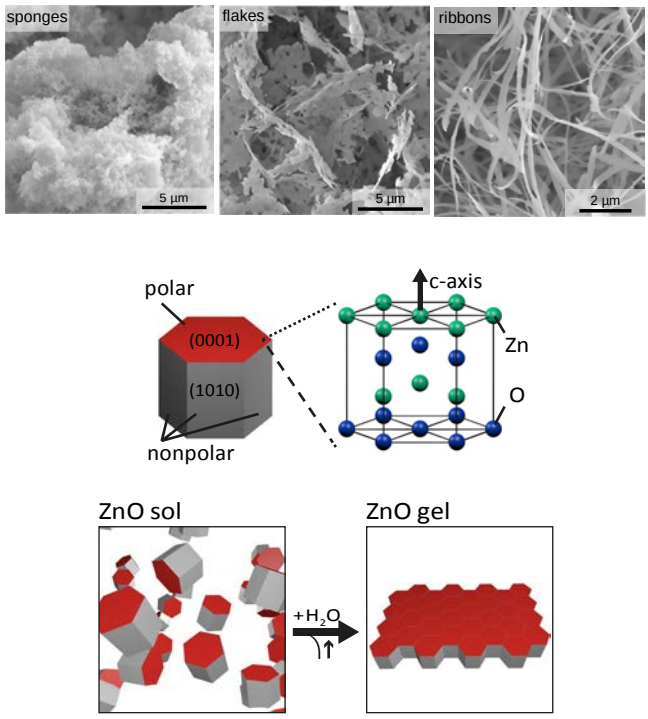


**Figure 23.** Depending on the destabilization conditions the morphology of the final aerogels can be tuned. Oriented attachment of initial nanoparticles due to changed solvent polarity.[142]

Recently the Eychmüller group managed to control the network morphology of the final aerogel through different destabilization routes.[142] Starting with a stable colloidal solution of ZnO nanoparticles in ethanol they achieved a sponge-like network by adding an oxidizing agent and two-dimensional structures (ribbons and flakes) by adding water (see Figure 23). While the first strategy is well known for a controlled destabilization and has been presented several times the second approach is novel. In this, water is responsible for the destabilization as well as for the formation of the two-dimensional secondary structures. Water has a more than three times higher dielectric constant than ethanol. Hence, the electrostatic repulsion of the charge stabilized ZnO nanoparticles decreases causing the destabilization. Besides, the increase in solvent polarity induces an oriented attachment of the aggregating particles in a way that non-polar facets will stick together just exposing the polar facets to the solution. Because of the hexagonal crystal structure of the ZnO nanoparticles a two-dimensional arrangement results (see Figure 23).

## Gels from carbon nanostructures

Already in its macroscopic allotropes, carbon is one of the most diverse among all elements. In particular, the discovery of the nanoscale allotropes fullerene, carbon nanotubes (CNTs) and graphene let to a revolution of carbon research.[143-148] This unique element stands out because of its diverse properties like electrical conductivity, low density and chemical inertness. Especially porous carbon materials like charcoal, carbide-derived carbons, Kroll carbons, mesoporous carbons obtained from silica templates and many more show extraordinary potential for applications in energy storage, energy conversion and catalysis.[149-155] Most of these materials are obtained through pyrolysis approaches starting from organic, bio, or polymer materials. Besides, many carbon aerogels can be obtained from pyrolysis of resorcinol-formaldehyde aerogels, which are produced via the classical polymerization gelation approach and comparable procedures.[156-159] Recent developments also focus on the use of biomass starting materials to obtain carbon aerogels.[160,161]

In 2007 the first CNT aerogels synthesized from a CNT suspension were reported.[162] The final gels were obtained through freeze drying and showed a high mechanical strength, supporting loads 8000 times their weight and were electrically conductive. Ultra light multi-walled CNT (MWCNT) aerogels could be obtained from the gelation of silylether-modified MWCNTs with a density of just 4 mg/cm$^3$.[163] Theses aerogels show a pressure sensitive electrical resistance and could be applied for chloroform vapor sensing.

**Figure 24.** Aerographene is the record holding material with the lowest density.[164]

A prototype all solid-state supercapacitor based on nitrogen and boron co-doped graphene aerogels was reported by the Müllen group in 2012.[165] They obtained the aerogel by a hydrothermal reductive treatment of GO with $NH_3BF_3$ followed by freeze-drying. One year later the material with the lowest density known to date was discovered and it was fabricated from CNTs and graphene sheets (see Figure 24).[164] This material, also known as aerographene, is electrically conductive, has a high absorption capacity und shows an outstanding temperature-invariant elasticity. Another method to obtain graphene aerogels was

introduced in the same year by a different group.[166] They started from GO in an ethylenediamine aqueous solution. A subsequent microwave treatment induced the formation of the graphene gel that could be transformed into an aerogel via freeze-drying. This material shows an outstandingly reversible compressibility, recovering fully after a 90 % compression. Further studies on graphene aerogels focused on the investigation of the gel formation mechanism, the applicability as supercapacitors and the extraordinary mechanical properties, respectively.[167-169] The interested reader can find a more detailed overview on aerogels made from CNTs and graphene elsewhere.[170-173]

## Gels from hybrid nanostructures

Starting with pre-formed nanoparticles proved to be beneficial for the synthesis of hybrid materials. Since the gelation mechanism is mainly determined by the stabilizers of the nanoparticles, different materials can easily be combined as long as the surface chemistry is comparable. The Eychmüller group prepared Au and CdTe nanoparticles both stabilized with either TGA or a tetrazole stabilizer to assemble them into mixed aerogels.[174,175] Using the photooxidation approach they successfully produced mixed CdTe/Au aerogels with adjustable emission properties (see Figure 25 A). In this the expected quenching of the luminescence for increasing Au content is observed in the macroscopic gels. This proves the uniform distribution of the Au and CdTe nanoparticles in the network. Similar results were reported for mixed tetrazole stabilized Au and CdTe nanoparticle gels (see Figure 25 B). With increasing Au content the luminescence decreased and shifted to lower energies while the photoluminescence lifetime was significantly decreased as expected for the quenching process.

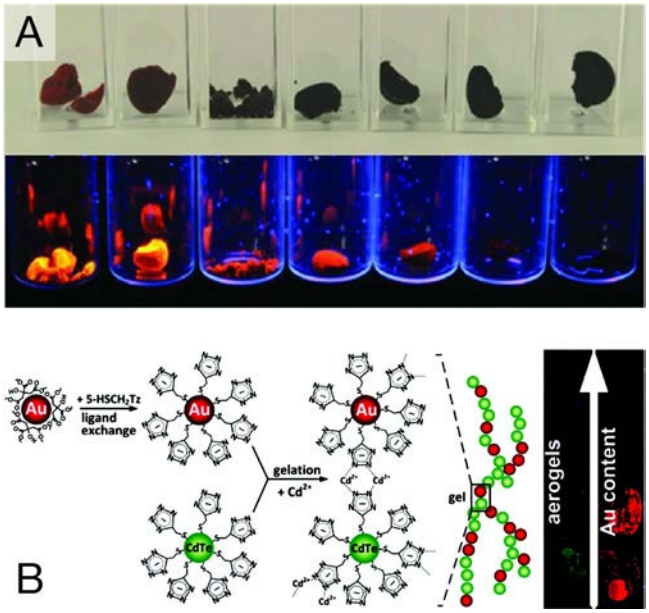


**Figure 25.** Gradual mixing of the aerogel composition from pure CdTe to pure Au aerogel. (A) Pure and hybrid gels were obtained by photooxidation of the mixed Au and CdTe colloids.**[174]** (B) Linking tetrazole stabilized CdTe and Au nanoparticles with $Cd^{2+}$-ions into gel structures.**[175]**

The Arachchige group recently demonstrated the formation of CdSe/Ag aerogels by co-gelation of the thiol-stabilized precursor particles with the help of the oxidizing agent NMO.[176] In contrast to CdSe/Au hybrid gels, where luminescence quenching was the dominant effect, they found a new emission channel in between the band edge and the trap state emission of the CdSe nanoparticles. They explain this different behavior by more favorable interfacial chemical bonds at the CdSe/Ag interface compared to Au and a consequent intermixing of the electronic states.

A different approach to metal/semiconductor hybrid aerogels was reported by the Hope-Weeks group.[177,178] In this they already started with either Au or Ag modified CdS nanoparticles that were assembled into gel structures by the addition of an oxidizing agent. The metal content was found to have a substantial influence on the emission properties as well as on the gel-formation kinetics.

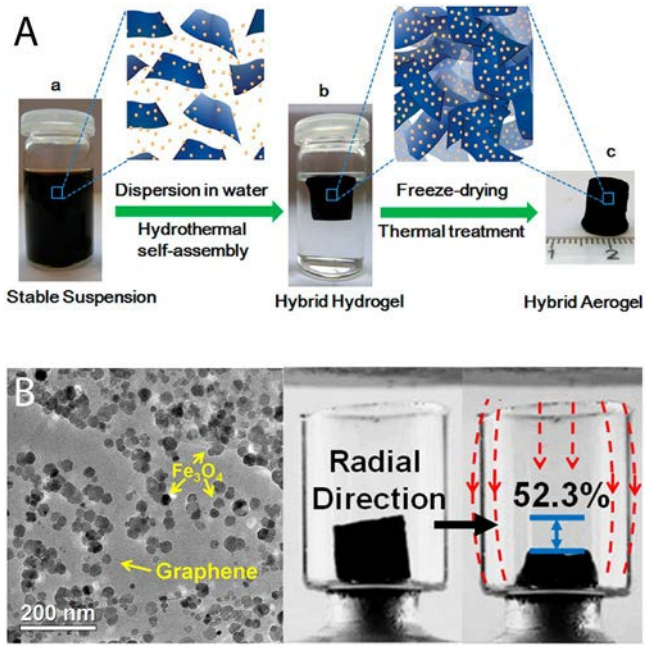


**Figure 26.** Formation mechanism of hybrid graphene/metal oxide aerogels (A).[179] Deformation of graphene/iron oxide aerogel in external magnetic field (B).[180]

Another smart way to produce hybrid aerogels was reported by several groups where they incorporated metal oxide nanoparticles into a graphene aerogel (see Figure 26 A).[179-183] In this they start from a stable suspension of GO and the respective metal oxide nanoparticles in water and subsequently reduce the GO to rGO/graphene. Since the polarity changes from GO (hydrophilic) to graphene (hydrophobic) the carbon sheets assemble into a three-dimensional network incorporating the other nanoparticles present. The incorporation of magnetite nanoparticles into the gel-network introduces magnetic properties to the final aerogels (see Figure 26 B). It could be shown that the morphology and the resistivity of the composite aerogel can be changed reversibly by changing the surrounding magnetic field.[180] Due to the electrical conductivity of the graphene scaffold, these materials are furthermore very promising for applications as electrodes in lithium ion batteries and for the electrocatalytic ORR, respectively.[179,181,182] Another approach yielded $Fe_2O_3$/graphene aerogels by the in situ iron oxide nanoparticle formation during the hydrothermal assembly into the gel network.[184] This material showed an outstanding durability and rate performance when used as anodes in lithium ion batteries. A different work following the same synthetic approach yielded iron

oxide/graphene aerogels that show promising adsorption capacities for oil and heavy metal ion removal from waste-water.[185] Using graphene aerogels, which were obtained from the reduction of GO, as a template, the Müllen group produced a graphene/silica hybrid aerogel that furthermore could be decorated with metal oxide particles.[186] These materials show excellent supercapacitive performances. Ternary hybrid aerogels made from GO, NiFe-layered double hydroxide and N-deficient porous $C_3N_4$, obtained from a hydrothermal co-destabilization approach, showed great potential for the photoelectrochemical water oxidation.[187]

The Niederberger group produced several oxide-based hybrid aerogels.[188-190] Starting from trizma functionalized $TiO_2$ nanoparticles in water, which can be destabilized by annealing to form a three-dimensional network, they incorporated either Au, $Fe_3O_4$ or Au and $WO_x$ nanoparticles into the anatase gel structure. For the Au/$TiO_2$ hybrid aerogels they reported a good photocatalytic degradation of a rhodamine dye under artificial sunlight illumination.[188] Using the same approach they produced magnetite/anatase hybrid gels with different loadings and could show a structured phase separation when the assembly was conducted in an external magnetic field.[189] For the ternary mixed aerogels they reported an excellent photocatalytic activity in the degradation of methylene blue.[190]

## DNA Origami aerogels

To date aerogels made of DNA or DNA origami building blocks have not been reported. This is probably manly because of the still very expensive access to DNA nanostructures. However, since nanostructures made of DNA offer an extreme amount of control this is a very promising class of materials whose potential we want to emphasize. DNA origami are two- or three-dimensional nanostructures made of DNA with full programmable shape control.[191,192] The structures itself are purely made of organic material. However, they can serve to precisely attach and arrange inorganic nanoparticles.[193,194] Furthermore, it has been shown that origami nanostructures can be used as a template to cast inorganic nano objects with a defined shape.[195-197] The Seidel group even showed that the inorganic nanostructures obtained still have an intact DNA shell, which makes it possible to assemble them in a controlled manner.[197] So far, several approaches to assemble DNA origami building blocks into larger structures have been shown and some of them already resemble gel-like structures (see Figure 27).[198,199]

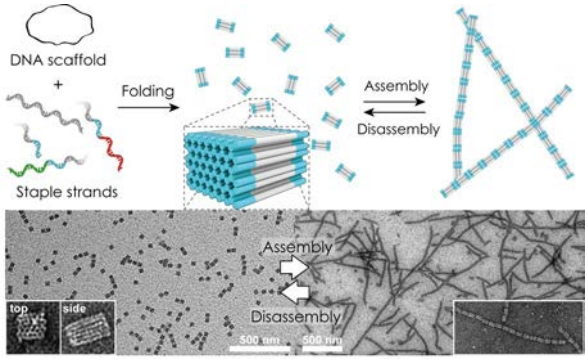


**Figure 27.** Three-dimensional assembly made of DNA origami building blocks.[199]

Another approach to assemble pre-formed nanoparticles has been studied extensively by the Mirkin group. They Single stranded DNA as stabilizers of different nanostructures to attach them to each other and assemble them into certain super-structures.[200,201] However, since the particles are functionalized uniformly the possibilities of directional assembly are limited, whereas in DNA origami structures every surface can be functionalized with a unique motive making them much more flexible for certain assembly purposes.

## Conclusions and Perspectives

currently materials, properties investigated

start to use this approach to specifically solve problems/address application

major benefits, self-supporting metal aerogels for electrocatalysis.

## References


[1] S. S. Kistler, *Nature* **1931**, *127*, 741–741.

[2] J. V. Alemán, A. V. Chadwick, J. He, M. Hess, K. Horie, R. G. Jones, P. Kratochvíl, I. Meisel, I. Mita, G. Moad, et al., *Pure and Applied Chemistry* **2007**, *79*, 1–29.

[3] N. Hüsing, U. Schubert, *Angew. Chem. Int. Ed.* **1998**, *37*, 22–45.

[4] A. C. Pierre, G. M. Pajonk, *Chem. Rev.* **2002**, *102*, 4243–4266.

[5] M. A. Aegerter, N. Leventis, M. M. Koebel, *Aerogels Handbook*, Springer Science & Business Media, **2011**.

[6] M. Nič, J. Jirát, B. Košata, A. Jenkins, A. McNaught, Eds., *IUPAC Compendium of Chemical Terminology*, Iupac, Research Triagle Park, NC, **2009**.

[7] L. Ren, S. Cui, F. Cao, Q. Guo, *Angew. Chem. Int. Ed.* **2014**, *53*, 10147–10149.

*[8]* A. Pons, L. Casas, E. Estop, E. Molins, K. D. M. Harris, M. Xu, *J. Non-Cryst. Solids* **2012**, *358*, 461–469.

[9] B. Ding, J. Cai, J. Huang, L. Zhang, Y. Chen, X. Shi, Y. Du, S. Kuga, *J. Mater. Chem.* **2012**, *22*, 5801–9.

[10] I. Coropceanu, M. G. Bawendi, *Nano Lett.* **2014**, *14*, 4097–4101.

[11] F. Meinardi, A. Colombo, K. A. Velizhanin, R. Simonutti, M. Lorenzon, L. Beverina, R. Viswanatha, V. I. Klimov, S. Brovelli, *Nature Photon* **2014**, *8*, 392–399.

[12] L. R. Bradshaw, K. E. Knowles, S. McDowall, D. R. Gamelin, *Nano Lett.* **2015**, *15*, 1315–1323.

[13] T. Otto, M. Müller, P. Mundra, V. Lesnyak, H. V. Demir, N. Gaponik, A. Eychmüller, *Nano Lett.* **2012**, *12*, 5348–5354.

[14] A. Benad, C. Guhrenz, C. Bauer, F. Eichler, M. Adam, C. Ziegler, N. Gaponik, A. Eychmüller, *ACS Appl. Mater. Interfaces* **2016**, *8*, 21570–21575.

[15] M. Adam, N. Gaponik, A. Eychmüller, T. Erdem, Z. Soran-Erdem, H. V. Demir, *J. Phys. Chem. Lett.* **2016**, *7*, 4117–4123.

[16] M. L. Anderson, C. A. Morris, R. M. Stroud, C. I. Merzbacher, D. R. Rolison, **1999**, *15*, 674–681.

[17] C. Morris, M. Anderson, R. Stroud, C. Merzbacher, D. Rolison, *Science* **1999**, *284*, 622–624.

[18] N. Leventis, I. A. Elder, D. R. Rolison, M. L. Anderson, C. I. Merzbacher, *Chem. Mater.* **1999**, *11*, 2837–2845.

[19] L. Sorensen, G. F. Strouse, A. E. Stiegman, *Adv. Mater.* **2006**, *18*, 1965–1967.

[20] Q. Wang, N. Iancu, D.-K. Seo, *Chem. Mater.* **2005**, *17*, 4762–4764.

[21] R. Wang, G. Li, Y. Dong, Y. Chi, G. Chen, *Anal. Chem.* **2013**, *85*, 8065–8069.

[22] F. A. Inam, M. D. W. Grogan, M. Rollings, T. Gaebel, J. M. Say, C. Bradac, T. A. Birks, W. J. Wadsworth, S. Castelletto, J. R. Rabeau, et al., *ACS Nano* **2013**, *7*, 3833–3843.

[23] M. Aghajamali, M. Iqbal, T. K. Purkait, L. Hadidi, R. Sinelnikov, J. G. C. Veinot, *Chem. Mater.* **2016**, *28*, 3877–3886.

[24] J. Cai, S. Kimura, M. Wada, S. Kuga, *Biomacromolecules* **2009**, *10*, 87–94.

[25] Y. Chen, K. C. Ng, W. Yan, Y. Tang, W. Cheng, *RSC Adv.* **2011**, *1*, 1265.

[26] P. A. DeSario, J. J. Pietron, D. E. DeVantier, T. H. Brintlinger, R. M. Stroud, D. R. Rolison, *Nanoscale* **2013**, *5*, 8073–11.

[27] J. L. Mohanan, S. L. Brock, *J. Non-Cryst. Solids* **2004**, *350*, 1–8.

[28] J. L. Mohanan, I. U. Arachchige, S. L. Brock, *Science* **2005**, *307*, 397–400.

[29] Z. Qi, J. Weissmüller, *ACS Nano* **2013**, *7*, 5948–5954.

[30] J. Biener, A. Wittstock, L. A. Zepeda-Ruiz, M. M. Biener, V. Zielasek, D. Kramer, R. N. Viswanath, J. Weissmüller, M. Bäumer, A. V. Hamza, *Nat. Mater.* **2008**, *8*, 47–51.

[31] J. Erlebacher, M. J. Aziz, A. Karma, N. Dimitrov, K. Sieradzki, *Nature* **2001**, *410*, 450–453.

*[32]* R. C. Newman, S. G. Corcoran, J. Erlebacher, M. J. Aziz, K. Sieradzki, *MRS Bull.* **1999**, *24*, 24–28.

*[33]* N. Leventis, N. Chandrasekaran, C. Sotiriou-Leventis, A. Mumtaz, *J. Mater. Chem.* **2009**, *19*, 63–65.

[34] N. Leventis, N. Chandrasekaran, A. G. Sadekar, S. Mulik, C. Sotiriou-Leventis, *J. Mater. Chem.* **2010**, *20*, 7456–16.

[35] S. Mahadik-Khanolkar, S. Donthula, A. Bang, C. Wisner, C. Sotiriou-Leventis, N. Leventis, *Chem. Mater.* **2014**, *26*, 1318–1331.

[36] B. C. Tappan, S. A. Steiner III, E. P. Luther, *Angew. Chem. Int. Ed.* **2010**, *49*, 4544–4565.

[37] H. C. Shin, J. Dong, M. Liu, *Adv. Mater.* **2003**, *15*, 1610–1614.

[38] H.-C. Shin, M. Liu, *Chem. Mater.* **2004**, *16*, 5460–5464.

[39] X. Chen, C.-H. Cui, Z. Guo, J.-H. Liu, X.-J. Huang, S.-H. Yu, *Small* **2011**, *7*, 858–863.

[40] A.-K. Herrmann, P. Formanek, L. Borchardt, M. Klose, L. Giebeler, J. Eckert, S. Kaskel, N. Gaponik, A. Eychmüller, *Chem. Mater.* **2014**, *26*, 1074–1083.

[41] N. C. Bigall, A.-K. Herrmann, M. Vogel, M. Rose, P. Simon, W. Carrillo-Cabrera, D.

Dorfs, S. Kaskel, N. Gaponik, A. Eychmüller, *Angew. Chem. Int. Ed.* **2009**, *48*, 9731–9734.

[42] L. Kühn, A.-K. Herrmann, B. Rutkowski, M. Oezaslan, M. Nachtegaal, M. Klose, L. Giebeler, N. Gaponik, J. Eckert, T. J. Schmidt, et al., *Chem. Eur. J.* **2016**, *22*, 13446–13450.

[43] T. Shibata, B. A. Bunker, Z. Zhang, D. Meisel, C. F. Vardeman, J. D. Gezelter, *J. Am. Chem. Soc.* **2002**, *124*, 11989–11996.

[44] D. F. Swearer, H. Zhao, L. Zhou, C. Zhang, H. Robatjazi, J. M. P. Martirez, C. M. Krauter, S. Yazdi, M. J. McClain, E. Ringe, et al., *Proc. Natl. Acad. Sci. U.S.A.* **2016**, *113*, 8916–8920.

*[45]* Y. Tang, K. L. Yeo, Y. Chen, L. W. Yap, W. Xiong, W. Cheng, *J. Mater. Chem. A* **2013**, *1*, 6723–4.

[46] H.-L. Gao, L. Xu, F. Long, Z. Pan, Y.-X. Du, Y. Lu, J. Ge, S.-H. Yu, *Angew. Chem. Int. Ed.* **2014**, *53*, 4561–4566.

*[47]* S. M. Jung, D. J. Preston, H. Y. Jung, Z. Deng, E. N. Wang, J. Kong, *Adv. Mater.* **2015**, *28*, 1413–1419.

[48] A. Freytag, S. Sánchez-Paradinas, S. Naskar, N. Wendt, M. Colombo, G. Pugliese, J. Poppe, C. Demirci, I. Kretschmer, D. W. Bahnemann, et al., *Angew. Chem. Int. Ed.* **2016**, *55*, 1200–1203.

[49] K. G. S. Ranmohotti, X. Gao, I. U. Arachchige, *Chem. Mater.* **2013**, *25*, 3528–3534.

[50] B. Cai, D. Wen, W. Liu, A.-K. Herrmann, A. Benad, A. Eychmüller, *Angew. Chem. Int. Ed.* **2015**, *54*, 13101–13105.

*[51]* X. Gao, R. J. Esteves, T. T. H. Luong, R. Jaini, I. U. Arachchige, *J. Am. Chem. Soc.* **2014**, *136*, 7993–8002.

[52] X. Gao, R. J. A. Esteves, L. Nahar, J. Nowaczyk, I. U. Arachchige, *ACS Appl. Mater. Interfaces* **2016**, acsami.5b11582–10.

[53] W. Liu, A.-K. Herrmann, D. Geiger, L. Borchardt, F. Simon, S. Kaskel, N. Gaponik, A. Eychmüller, *Angew. Chem. Int. Ed.* **2012**, *51*, 5743–5747.

[54] W. Liu, P. Rodriguez, L. Borchardt, A. Foelske, J. Yuan, A.-K. Herrmann, D. Geiger, Z. Zheng, S. Kaskel, N. Gaponik, et al., *Angew. Chem. Int. Ed.* **2013**, *52*, 9849–9852.

[55] W. Liu, A.-K. Herrmann, N. C. Bigall, P. Rodriguez, D. Wen, M. Oezaslan, T. J. Schmidt, N. Gaponik, A. Eychmüller, *Acc. Chem. Res.* **2015**, *48*, 154–162.

[56] A. Rabis, P. Rodriguez, T. J. Schmidt, *ACS Catal.* **2012**, *2*, 864–890.

[57] D. Wen, W. Liu, D. Haubold, C. Zhu, M. Oschatz, M. Holzschuh, A. Wolf, F. Simon,

S. Kaskel, A. Eychmüller, *ACS Nano* **2016**, *10*, 2559–2567.

[58] C. Zhu, D. Wen, M. Oschatz, M. Holzschuh, W. Liu, A.-K. Herrmann, F. Simon, S. Kaskel, A. Eychmüller, *Small* **2014**, *11*, 1430–1434.

[59] V. R. Stamenkovic, B. S. Mun, M. Arenz, K. J. J. Mayrhofer, C. A. Lucas, G. Wang, P. N. Ross, N. M. Markovic, *Nat. Mater.* **2007**, *6*, 241–247.

[60] Y. Cai, R. R. Adzic, *Advances in Physical Chemistry* **2011**, *2011*, 1–16.

*[61]* J. Zhang, M. B. Vukmirovic, Y. Xu, M. Mavrikakis, R. R. Adzic, *Angew. Chem.* **2005**, *117*, 2170–2173.

[62] V. Stamenkovic, B. S. Mun, K. J. J. Mayrhofer, P. N. Ross, N. M. Markovic, J. Rossmeisl, J. Greeley, J. K. Nørskov, *Angew. Chem. Int. Ed.* **2006**, *45*, 2897–2901.

[63] V. Viswanathan, H. A. Hansen, J. Rossmeisl, J. K. Nørskov, *ACS Catal.* **2012**, *2*, 1654–1660.

[64] W. Liu, D. Haubold, B. Rutkowski, M. Oschatz, R. Hübner, M. Werheid, C. Ziegler, L. Sonntag, S. Liu, Z. Zheng, et al., *Chem. Mater.* **2016**, *28*, 6477–6483.

[65] D. Wen, A.-K. Herrmann, L. Borchardt, F. Simon, W. Liu, S. Kaskel, A. Eychmüller, *J. Am. Chem. Soc.* **2014**, *136*, 2727–2730.

[66] D. Wen, W. Liu, A.-K. Herrmann, A. Eychmüller, *Chem. Eur. J.* **2014**, *20*, 4380–4385.

[67] A. Heller, *Phys Chem Chem Phys* **2004**, *6*, 209–8.

[68] J. A. Cracknell, K. A. Vincent, F. A. Armstrong, *Chem. Rev.* **2008**, *108*, 2439–2461.

[69] L. Halámková, J. Halámek, V. Bocharova, A. Szczupak, L. Alfonta, E. Katz, *J. Am. Chem. Soc.* **2012**, *134*, 5040–5043.

[70] I. Willner, Y. M. Yan, B. Willner, R. Tel-Vered, *Fuel Cells* **2009**, *9*, 7–24.

[71] P. Kavanagh, D. Leech, *Phys Chem Chem Phys* **2013**, *15*, 4859–11.

[72] X.-Y. Yang, G. Tian, N. Jiang, B.-L. Su, *Energy Environ. Sci.* **2012**, *5*, 5540–5563.

[73] N. Zheng, X. Bu, B. Wang, P. Feng, *Science* **2002**, *298*, 2366–2369.

[74] H. Li, A. Laine, M. O'Keeffe, O. M. Yaghi, *Science* **1999**, *283*, 1145–1147.

[75] N. F. Zheng, X. H. Bu, P. Y. Feng, *Nature* **2003**, *426*, 428–432.

[76] Y. A. Vlasov, N. Yao, D. J. Norris, *Adv. Mater.* **1999**, *11*, 165–169.

*[77]* W. Park, J. S. King, C. W. Neff, C. Liddell, C. J. Summers, *Phys. Status Solidi B* **2002**, *229*, 949–960.

*[78]* C. B. Murray, C. R. Kagan, M. G. Bawendi, *Annual Review of Materials Science* **2000**, *30*, 545–610.

[79] C. B. Murray, C. R. Kagan, M. G. Bawendi, *Science* **1995**.

[80] I. U. Arachchige, J. L. Mohanan, S. L. Brock, *Chem. Mater.* **2005**, *17*, 6644–6650.

[81] I. U. Arachchige, S. L. Brock, *J. Am. Chem. Soc.* **2006**, *128*, 7964–7971.

[82] Q. Yao, I. U. Arachchige, S. L. Brock, *J. Am. Chem. Soc.* **2009**, *131*, 2800–2801.

[83] I. U. Arachchige, S. L. Brock, *J. Am. Chem. Soc.* **2007**, *129*, 1840–1841.

[84] H. Yu, S. L. Brock, *ACS Nano* **2008**, *2*, 1563–1570.

[85] H. Yu, R. Bellair, R. M. Kannan, S. L. Brock, *J. Am. Chem. Soc.* **2008**, *130*, 5054–5055.

[86] H. Yu, Y. Liu, S. L. Brock, *ACS Nano* **2009**, *3*, 2000–2006.

[87] L. Korala, S. L. Brock, *J. Phys. Chem. C* **2012**, *116*, 17110–17117.

*[88]* N. Gaponik, A. Wolf, R. Marx, V. Lesnyak, K. Schilling, A. Eychmüller, *Adv. Mater.* **2008**, *20*, 4257–4262.

[89] H. Chen, V. Lesnyak, N. C. Bigall, N. Gaponik, A. Eychmüller, *Chem. Mater.* **2010**, *22*, 2309–2314.

[90] S. Sekiguchi, K. Niikura, N. Iyo, Y. Matsuo, A. Eguchi, T. Nakabayashi, N. Ohta, K. Ijiro, *ACS Appl. Mater. Interfaces* **2011**, *3*, 4169–4173.

*[91]* I. R. Pala, I. U. Arachchige, D. G. Georgiev, S. L. Brock, *Angew. Chem. Int. Ed.* **2010**, *49*, 3661–3665.

[92] V. Lesnyak, S. V. Voitekhovich, P. N. Gaponik, N. Gaponik, A. Eychmüller, *ACS Nano* **2010**, *4*, 4090–4096.

[93] A. Wolf, V. Lesnyak, N. Gaponik, A. Eychmüller, *J. Phys. Chem. Lett.* **2012**, *3*, 2188–2193.

[94] C. Rengers, S. V. Voitekhovich, S. Kittler, A. Wolf, M. Adam, N. Gaponik, S. Kaskel, A. Eychmüller, *Nanoscale* **2015**, *7*, 12713–12721.

[95] S.-H. Jeong, J. W. Lee, D. Ge, K. Sun, T. Nakashima, S. I. Yoo, A. Agarwal, Y. Li, N. A. Kotov, *J. Mater. Chem.* **2011**, *21*, 11639–5.

[96] Q. Yao, S. L. Brock, *Inorg. Chem.* **2011**, *50*, 9985–9992.

[97] S. Sánchez-Paradinas, D. Dorfs, S. Friebe, A. Freytag, A. Wolf, N. C. Bigall, *Adv. Mater.* **2015**, *27*, 6152–6156.

[98] S. Naskar, J. F. Miethe, S. Sánchez-Paradinas, N. Schmidt, K. Kanthasamy, P. Behrens, H. Pfnür, N. C. Bigall, *Chem. Mater.* **2016**, *28*, 2089–2099.

[99] V. Sayevich, B. Cai, A. Benad, D. Haubold, L. Sonntag, N. Gaponik, V. Lesnyak, A. Eychmüller, *Angew. Chem. Int. Ed.* **2016**, *55*, 6334–6338.

[100] A. Singh, B. A. Lindquist, G. K. Ong, R. B. Jadrich, A. Singh, H. Ha, C. J. Ellison, T. M. Truskett, D. J. Milliron, *Angew. Chem.* **2015**, *127*, 15053–15057.

[101] V. Sayevich, C. Guhrenz, M. Sin, V. M. Dzhagan, A. Weiz, D. Kasemann, E. Brunner, M. Ruck, D. R. T. Zahn, K. Leo, et al., *Adv. Funct. Mater.* **2016**, *26*, 2163–2175.

[102] J. N. De Freitas, L. Korala, L. X. Reynolds, S. A. Haque, S. L. Brock, A. F. Nogueira, *Phys Chem Chem Phys* **2012**, *14*, 15180–5.

[103] L. Korala, Z. Wang, Y. Liu, S. Maldonado, S. L. Brock, *ACS Nano* **2013**, *7*, 1215–1223.

[104] L. Korala, L. Li, S. L. Brock, *Chem. Commun.* **2012**, *48*, 8523–3.

[105] J. Yuan, D. Wen, N. Gaponik, A. Eychmüller, *Angew. Chem. Int. Ed.* **2012**, *52*, 976–979.

[106] I. R. Pala, S. L. Brock, *ACS Appl. Mater. Interfaces* **2012**, *4*, 2160–2167.

[107] S. Ganguly, C. Zhou, D. Morelli, J. Sakamoto, S. L. Brock, *J. Phys. Chem. C* **2012**, *116*, 17431–17439.

[108] S. Ganguly, S. L. Brock, *J. Mater. Chem.* **2011**, *21*, 8800–7.

[109] S. Bag, P. N. Trikalitis, P. J. Chupas, G. S. Armatas, M. G. Kanatzidis, *Science* **2007**, *317*, 490–493.

[110] S. Bag, I. U. Arachchige, M. G. Kanatzidis, *J. Mater. Chem.* **2008**, *18*, 3628.

[111] K. S. Subrahmanyam, C. D. Malliakas, S. M. Islam, D. Sarma, J. Wu, M. G. Kanatzidis, *Chem. Mater.* **2016**, *28*, 7744–7749.

[112] S. Bag, A. F. Gaudette, M. E. Bussell, M. G. Kanatzidis, *Nature Chem* **2009**, *1*, 217–224.

[113] S. Bag, M. G. Kanatzidis, *J. Am. Chem. Soc.* **2010**, *132*, 14951–14959.

[114] B. J. Riley, J. Chun, J. V. Ryan, J. Matyas, X. S. Li, D. W. Matson, S. K. Sundaram, D. M. Strachan, J. D. Vienna, *RSC Adv.* **2011**, *1*, 1704–12.

[115] Y. Oh, S. Bag, C. D. Malliakas, M. G. Kanatzidis, *Chem. Mater.* **2011**, *23*, 2447–2456.

[116] B. J. Riley, J. Chun, W. Um, W. C. Lepry, J. Matyas, M. J. Olszta, X. Li, K. Polychronopoulou, M. G. Kanatzidis, *Environ. Sci. Technol.* **2013**, *47*, 7540–7547.

[117] K. S. Subrahmanyam, C. D. Malliakas, D. Sarma, G. S. Armatas, J. Wu, M. G. Kanatzidis, *J. Am. Chem. Soc.* **2015**, *137*, 13943–13948.

[118] B. J. Riley, D. A. Pierce, W. C. Lepry, J. O. Kroll, J. Chun, K. S. Subrahmanyam, M. G. Kanatzidis, F. K. Alblouwy, A. Bulbule, E. M. Sabolsky, *Ind. Eng. Chem. Res.* **2015**, *54*, 11259–11267.

[119] A. Feinle, N. Hüsing, *The Journal of Supercritical Fluids* **2015**, *106*, 2–8.

[120] A. Soleimani Dorcheh, M. H. Abbasi, *Journal of Materials Processing Technology* **2008**, *199*, 10–26.

[121] J. P. Randall, M. A. B. Meador, S. C. Jana, *ACS Appl. Mater. Interfaces* **2011**, *3*, 613–626.

[122] T. F. Baumann, A. E. Gash, S. C. Chinn, A. M. Sawvel, R. S. Maxwell, J. H. Satcher, *Chem. Mater.* **2005**, *17*, 395–401.

[123] C. Laberty-Robert, J. W. Long, E. M. Lucas, K. A. Pettigrew, R. M. Stroud, M. S. Doescher, D. R. Rolison, *Chem. Mater.* **2006**, *18*, 50–58.

[124] Y. P. Gao, C. N. Sisk, L. J. Hope-Weeks, *Chem. Mater.* **2007**, *19*, 6007–6011.

[125] M. Davis, W. M. Hikal, C. Gümeci, L. J. Hope-Weeks, *Catal. Sci. Technol.* **2012**, *2*, 922.

[126] T. M. Fears, C. Sotiriou-Leventis, J. G. Winiarz, N. Leventis, *J Sol-Gel Sci Technol* **2015**, *77*, 244–256.

[127] D. R. Rolison, B. Dunn, *J. Mater. Chem.* **2001**, *11*, 963–980.

[128] G. Ozouf, C. Beauger, *J Mater Sci* **2016**, *51*, 5305–5320.

[129] G. Zu, J. Shen, L. Zou, W. Wang, Y. Lian, Z. Zhang, A. Du, *Chem. Mater.* **2013**, *25*, 4757–4764.

[130] N. Leventis, C. Sotiriou-Leventis, G. Zhang, A.-M. M. Rawashdeh, *Nano Lett.* **2002**, *2*, 957–960.

[131] N. Leventis, *Acc. Chem. Res.* **2007**, *40*, 874–884.

[132] G. Zhang, A. Dass, A.-M. M. Rawashdeh, J. Thomas, J. A. Counsil, C. Sotiriou-Leventis, E. F. Fabrizio, F. Ilhan, P. Vassilaras, D. A. Scheiman, et al., *J. Non-Cryst. Solids* **2004**, *350*, 152–164.

[133] M. A. B. Meador, E. F. Fabrizio, F. Ilhan, A. Dass, G. Zhang, P. Vassilaras, J. C. Johnston, N. Leventis, *Chem. Mater.* **2005**, *17*, 1085–1098.

[134] J. T. Korhonen, P. Hiekkataipale, J. Malm, M. Karppinen, O. Ikkala, R. H. A. Ras, *ACS Nano* **2011**, *5*, 1967–1974.

[135] F. Rechberger, R. Städler, E. Tervoort, M. Niederberger, *J Sol-Gel Sci Technol* **2016**, 1–7.

[136] F. J. Heiligtag, N. Kränzlin, M. J. Süess, M. Niederberger, *J Sol-Gel Sci Technol* **2013**, *70*, 300–306.

[137] F. Rechberger, F. J. Heiligtag, M. J. Süess, M. Niederberger, *Angew. Chem. Int. Ed.* **2014**, *53*, 6823–6826.

[138] F. Rechberger, G. Ilari, M. Niederberger, *Chem. Commun.* **2014**, *50*, 13138–13141.

[139] W. Cheng, F. Rechberger, M. Niederberger, *ACS Nano* **2016**, *10*, 2467–2475.

[140] S. Chen, G. Liu, H. Yadegari, H. Wang, S. Z. Qiao, *J. Mater. Chem. A* **2015**, *3*, 2559–2563.

[141] Z. Liu, K. Xu, P. She, S. Yin, X. Zhu, H. Sun, *Chemical Science* **2016**, *7*, 1926–1932.

[142] C. Ziegler, S. Klosz, L. Borchardt, M. Oschatz, S. Kaskel, M. Friedrich, R. Kriegel, T. Keilhauer, M. Armbrüster, A. Eychmüller, *Adv. Funct. Mater.* **2015**, *26*, 1014–1020.

[143] H. W. Kroto, J. R. Heath, S. C. O'Brien, R. F. Curl, R. E. Smalley, *Nature* **1985**, *318*, 162–163.

[144] S. Iijima, *Nature* **1991**, *354*, 56–58.

[145] D. S. Bethune, C. H. Klang, M. S. de Vries, G. Gorman, R. Savoy, J. Vazquez, R. Beyers, *Nature* **1993**, *363*, 605–607.

[146] S. Iijima, T. Ichihashi, *Nature* **1993**, *363*, 603–605.

[147] H. P. Boehm, A. Clauss, G. O. Fischer, U. Hofmann, *Z. Anorg. Allg. Chem.* **1962**, *316*, 119–127.

[148] K. S. Novoselov, A. K. Geim, S. V. Morozov, D. Jiang, Y. Zhang, S. V. Dubonos, I. V. Grigorieva, A. A. Firsov, *Science* **2004**, *306*, 666–669.

[149] S. Evers, L. F. Nazar, *Acc. Chem. Res.* **2013**, *46*, 1135–1143.

[150] F. Béguin, V. Presser, A. Balducci, E. Frackowiak, *Adv. Mater.* **2014**, *26*, 2219–2251.

[151] A. D. Roberts, X. Li, H. Zhang, *Chem. Soc. Rev.* **2014**, *43*, 4341–16.

[152] Z. Yang, J. Ren, Z. Zhang, X. Chen, G. Guan, L. Qiu, Y. Zhang, H. Peng, *Chem. Rev.* **2015**, *115*, 5159–5223.

[153] M. Oschatz, S. Thieme, L. Borchardt, M. R. Lohe, T. Biemelt, J. Brückner, H. Althues, S. Kaskel, *Chem. Commun.* **2013**, *49*, 5832–3.

[154] V. Presser, M. Heon, Y. Gogotsi, *Adv. Funct. Mater.* **2011**, *21*, 810–833.

[155] J. Lee, J. Kim, T. Hyeon, *Adv. Mater.* **2006**, *18*, 2073–2094.

[156] C. Moreno-Castilla, F. J. Maldonado-Hódar, *Carbon* **2005**, *43*, 455–465.

[157] A. K. Meena, G. K. Mishra, P. K. Rai, C. Rajagopal, P. N. Nagar, *Journal of Hazardous Materials* **2005**, *122*, 161–170.

[158] N. Job, A. Théry, R. Pirard, J. Marien, L. Kocon, J.-N. Rouzaud, F. Béguin, J.-P. Pirard, *Carbon* **2005**, *43*, 2481–2494.

[159] M. Antonietti, N. Fechler, T.-P. Fellinger, *Chem. Mater.* **2014**, *26*, 196–210.

[160] X.-L. Wu, T. Wen, H.-L. Guo, S. Yang, X. Wang, A.-W. Xu, *ACS Nano* **2013**, *7*, 3589–3597.

[161] Y. Si, X. Wang, C. Yan, L. Yang, J. Yu, B. Ding, *Adv. Mater.* **2016**, 1–7.

[162] M. B. Bryning, D. E. Milkie, M. F. Islam, L. A. Hough, J. M. Kikkawa, A. G. Yodh, *Adv. Mater.* **2007**, *19*, 661–664.

[163] J. Zou, J. Liu, A. S. Karakoti, A. Kumar, D. Joung, Q. Li, S. I. Khondaker, S. Seal, L. Zhai, *ACS Nano* **2010**, *4*, 7293–7302.

[164] H. Sun, Z. Xu, C. Gao, *Adv. Mater.* **2013**, *25*, 2554–2560.

[165] Z.-S. Wu, A. Winter, L. Chen, Y. Sun, A. Turchanin, X. Feng, K. Müllen, *Adv. Mater.* **2012**, *24*, 5130–5135.

[166] H. Hu, Z. Zhao, W. Wan, Y. Gogotsi, J. Qiu, *Adv. Mater.* **2013**, *25*, 2219–2223.

[167] A. P. Goldstein, W. Mickelson, A. Machness, G. Lee, M. A. Worsley, L. Woo, A. Zettl, *J. Phys. Chem. C* **2014**, *118*, 28855–28860.

[168] Z.-Y. Sui, Y.-N. Meng, P.-W. Xiao, Z.-Q. Zhao, Z.-X. Wei, B.-H. Han, *ACS Appl. Mater. Interfaces* **2015**, *7*, 1431–1438.

[169] X. Xu, Q. Zhang, Y. Yu, W. Chen, H. Hu, H. Li, *Adv. Mater.* **2016**, 1–8.

[170] S. Nardecchia, D. Carriazo, M. L. Ferrer, M. C. Gutiérrez, F. del Monte, *Chem. Soc. Rev.* **2013**, *42*, 794–830.

[171] S. Araby, A. Qiu, R. Wang, Z. Zhao, C.-H. Wang, J. Ma, *J Mater Sci* **2016**, *51*, 9157–9189.

[172] V. Georgakilas, J. A. Perman, J. Tucek, R. Zboril, *Chem. Rev.* **2015**, *115*, 4744–4822.

[173] Z. Lin, Z. Zeng, X. Gui, Z. Tang, M. Zou, A. Cao, *Advanced Energy Materials* **2016**, *6*, 1600554–26.

[174] T. Hendel, V. Lesnyak, L. Kühn, A.-K. Herrmann, N. C. Bigall, L. Borchardt, S. Kaskel, N. Gaponik, A. Eychmüller, *Adv. Funct. Mater.* **2013**, *23*, 1903–1911.

[175] V. Lesnyak, A. Wolf, A. Dubavik, L. Borchardt, S. V. Voitekhovich, N. Gaponik, S. Kaskel, A. Eychmüller, *J. Am. Chem. Soc.* **2011**, *133*, 13413–13420.

[176] L. Nahar, R. J. A. Esteves, S. Hafiz, Ü. Özgür, I. U. Arachchige, *ACS Nano* **2015**, *9*, 9810–9821.

[177] S. K. Gill, L. J. Hope-Weeks, *Chem. Commun.* **2009**, 4384–3.

[178] S. K. Gill, P. Brown, L. J. Hope-Weeks, *J Sol-Gel Sci Technol* **2010**, *57*, 68–75.

[179] Z.-S. Wu, S. Yang, Y. Sun, K. Parvez, X. Feng, K. Müllen, *J. Am. Chem. Soc.* **2012**, *134*, 9082–9085.

[180] X. Xu, H. Li, Q. Zhang, H. Hu, Z. Zhao, J. Li, J. Li, Y. Qiao, Y. Gogotsi, *ACS Nano* **2015**, *9*, 3969–3977.

[181] W. Chen, S. Li, C. Chen, L. Yan, *Adv. Mater.* **2011**, *23*, 5679–5683.

[182] G. Zeng, N. Shi, M. Hess, X. Chen, W. Cheng, T. Fan, M. Niederberger, *ACS Nano* **2015**, *9*, 4227–4235.

[183] R. O. da Silva, F. J. Heiligtag, M. Karnahl, H. Junge, M. Niederberger, S. Wohlrab, *Catal. Today* **2015**, *246*, 101–107.

[184] L. Xiao, D. Wu, S. Han, Y. Huang, S. Li, M. He, F. Zhang, X. Feng, *ACS Appl. Mater. Interfaces* **2013**, *5*, 3764–3769.

[185] H.-P. Cong, X.-C. Ren, P. Wang, S.-H. Yu, *ACS Nano* **2012**, *6*, 2693–2703.

[186] Z.-S. Wu, Y. Sun, Y.-Z. Tan, S. Yang, X. Feng, K. Müllen, *J. Am. Chem. Soc.* **2012**, *134*, 19532–19535.

[187] Y. Hou, Z. Wen, S. Cui, X. Feng, J. Chen, *Nano Lett.* **2016**, *16*, 2268–2277.

[188] F. J. Heiligtag, M. D. Rossell, M. J. Süess, M. Niederberger, *J. Mater. Chem.* **2011**, *21*, 16893–7.

[189] F. J. Heiligtag, M. J. I. Airaghi Leccardi, D. Erdem, M. J. Süess, M. Niederberger, *Nanoscale* **2014**, *6*, 13213–13221.

[190] F. J. Heiligtag, W. Cheng, V. R. de Mendonça, M. J. Süess, K. Hametner, D. Günther, C. Ribeiro, M. Niederberger, *Chem. Mater.* **2014**, *26*, 5576–5584.

[191] P. W. K. Rothemund, *Nature* **2006**, *440*, 297–302.

[192] S. M. Douglas, H. Dietz, T. Liedl, B. Högberg, F. Graf, W. M. Shih, *Nature* **2009**, *459*, 414–418.

[193] R. Schreiber, J. Do, E.-M. Roller, T. Zhang, V. J. Schüller, P. C. Nickels, J. Feldmann, T. Liedl, *Nature Nanotech* **2013**, 1–5.

[194] A. Kuzyk, R. Schreiber, Z. Fan, G. Pardatscher, E.-M. Roller, A. Högele, F. C. Simmel, A. O. Govorov, T. Liedl, *Nature* **2012**, *483*, 311–314.

[195] R. Schreiber, S. Kempter, S. Holler, V. Schüller, D. Schiffels, S. S. Simmel, P. C. Nickels, T. Liedl, *Small* **2011**, *7*, 1795–1799.

[196] W. Sun, E. Boulais, Y. Hakobyan, W. L. Wang, A. Guan, M. Bathe, P. Yin, *Science* **2014**, *346*, 1258361–1258361.

[197] S. Helmi, C. Ziegler, D. J. Kauert, R. Seidel, *Nano Lett.* **2014**, *14*, 6693–6698.

[198] Y. Ke, L. L. Ong, W. M. Shih, P. Yin, *Science* **2012**, *338*, 1177–1183.

[199] T. Tigges, T. Heuser, R. Tiwari, A. Walther, *Nano Lett.* **2016**, DOI 10.1021/acs.nanolett.6b04146.

[200] C. A. Mirkin, R. L. Letsinger, R. C. Mucic, J. J. Storhoff, *Nature* **1996**, *382*, 607–609.

[201] J. I. Cutler, E. Auyeung, C. A. Mirkin, *J. Am. Chem. Soc.* **2012**, *134*, 1376–1391.